Carderock Division
Naval Surface Warfare Center
Bethesda, Md. 20084–5000

CARDIVNSWC–TR–61—93/12 March 1994
Survivability, Structures, and Materials Directorate
Technical Report

The Effects of Alloying Elements on the Strength and Cooling Rate Sensitivity of Ultra-Low Carbon Alloy Steel Weld Metals

by
M.G Vassilaros

The Effect of Alloying Elements on the Strength and Cooling Rate Sensitivity of Ultra-Low Carbon Alloy Steel Weld Metals

CARDIVNSWC–TR–61—93/12

Carderock Division
Naval Surface Warfare Center
Bethesda, Md. 20084–5000

CARDIVNSWC–TR–61—93/12 March 1994
Survivability, Structures, and Materials Directorate
Technical Report

The Effects of Alloying Elements on the Strength and Cooling Rate Sensitivity of Ultra-Low Carbon Alloy Steel Weld Metals

by
M.G. Vassilaros

CONTENTS

TABLES

Figures

Figures

ABSTRACT

A study was conducted to evaluate the effect of weld cooling rate on the strength of autogenous GTAW deposited weld metal. The basic weld metal composition was based on a low carbon bainite metallurgical system. The weld metal yield strength goal was 130 ksi, needed to surpass the current HY-130 weld metal requirements. Vacuum Induction Melted (VIM) heats of steel were produced and processed into 3/4" thickness plates. The autogenous gas tungsten arc welds (GTAW) on the parent steel plates were produced under two different heat input conditions. Tensile specimens were produced from the weldments; specimens from certain heats were subjected to gleeble thermal simulations of multi-pass welding conditions using the Gleeble 1500. All specimens were then evaluated for yield and ultimate tensile strength. From the data presented, it was found that the experimental compositions studied were less sensitive to cooling rate than current HY-130 welding consumables. The compositions tested approached the target yield strength of 130 ksi, but further work is necessary in this area.

ACKNOWLEDGMENTS

The author wishes to extend his gratitude to the other CDNSWC researchers who provided advice and assistance during the program. These people include, J. Blackburn, G. Franke, W. Worden, D. Meldrom, J. Nasso, A. Brandemarte and S. Womack. Additionally, the author acknowledges the large contribution of Ms. Denise Montiel to every aspect of this research.

ADMINISTRATIVE INFORMATION

This report covers the results of one in a series of weld wire chemistry studies conducted as part of the ULCB-130 Weld Wire program. The ULCB-130 program was sponsored by the SEAWOLF acquisition program of the Naval Sea Systems Command (PMS 350) under Program Element 64561N, Task Area 130-90.4, Fiscal Year 1989-91. The NAVSEA technical agent for the program was Mr. C. L. Null (05M2). The work was supervised by Mr. T. W. Montemarano, Head, Fatigue and Fracture Branch, Carderock Division, Naval Surface Warfare Center, Code 614. The report was prepared as part of the Low-Carbon Bainitic Weld Metal Program under the sponsorship of the Ship and Submarine Block Program (ND2B), Program Element 62234N, in Fiscal Year 1993. The Block Manager is Mr. I. L. Caplan, Carderock Division, Carderock Division Naval Surface Warfare Center, (Code 0115). The effort was supervised by Mr. R. DeNale, Carderock Division, Naval Surface Warfare Center, Code 615.

INTRODUCTION

This study was part of a program to develop new HY-130 welding consumables that are based on a low carbon bainite metallurgical system. The HY-130 steel system was developed as a weldable, quenched and tempered martensitic steel. The attainment of high strength and toughness in the as-welded condition of this steel requires careful control of the welding practice to maintain the proper high carbon martensite structure that produces these properties. This control requirement holds especially true for the weld metal.

The traditional approach to designing a weld metal for the HY-130 system has been to develop a martensitic material that can produce high strength and toughness in the as-welded condition (Dorschu and Lesnewich, 1964). Success in this approach requires the production of a quenched and tempered martensite structure in the weld. The quenching is provided by using low heat inputs to produce high cooling rates in the weld. The tempering occurs from the heating cycles of the subsequent weld passes. The as-deposited microstructure can be

very hard and sensitive to hydrogen cracking. To avoid this potential problem, a high preheat temperature can be applied to the weld to enhance the cracking resistance of this material (Linnert, 1967). Unfortunately, a preheating requirement for welding is costly and lowers productivity. The application of preheat also results in a reduction of the cooling rate in the weld. This condition further reduces the maximum allowed heat input that can produce a martensitic microstructure in the weld. However, it is possible to design a low carbon bainite weld system that has the required strength and toughness for welding HY-130 steel. The work of Pickering (Pickering, 1977) clearly showed that the strength of bainitic steels can be controlled by the metal chemistry alone without the need for stringent control of the cooling rate of the steel plate. This effect of chemistry control of strength has not been demonstrated for low-carbon bainitic weld metals. Such a weld metal would have the advantage of being less sensitive to cooling rate than current HY-130 consumables, and therefore would be more efficient for high heat input welding. Research at DTRC (currently CDNSWC) and the University of Pittsburgh has shown that bainitic steel is capable of strengths in the range from 80 to 140+ ksi yield strength (Garcia, 1991). This research has also shown that a fine austenite grain size and low inclusion content will enhance the toughness of steels. The purpose of this initial study was to assess the strength potential and cooling rate sensitivity of a series of bainitic weld metal compositions that were chosen as model materials for the HY-130 weld consumables development program. The overall program goal was to develop a bainitic welding consumable for gas-metal-arc welding (GMAW) HY-130 steel that would maintain desired properties up to heat input of 100 kJ/in. The program approach will include the development of the data needed to predict the effects of the various alloying elements on the strength, cooling rate sensitivity, and Charpy impact toughness of low carbon bainitic weld metal. The data will be used to produce a series of "candidate systems" each based on a different alloying philosophy that will be evaluated for

welding HY-130 steel. The evaluation of the "candidate systems" will include strength, CVN and DT impact toughness, hydrogen cracking susceptibility, and stress corrosion cracking (SCC) resistance. The data from the evaluation of the "candidate systems" will be used to formulate candidate GMA weld wire chemistries for HY-130 steel.

This report concerns the initial phase of the low-carbon bainitic weld wire program. The objective was to measure the effects of various alloy additions on the strength and cooling rate sensitivity of low-carbon weld metal (model materials).

MATERIALS

The model chemistries for this study were ultra-low-carbon compositions with a bainitic microstructure(ULCB steel). The chemistries were formulated with a goal of attaining a 130 ksi minimum yield strength while maintaining the desired bainitic microstructure. The target chemistries chosen for evaluation are given in Table 1.

The alloys were produced by USS Technical Center, Monroeville, Pennsylvania. The 22 heats of model materials were cast from 8 heats (300 pounds each) of vacuum induction melted (VIM) steel. The initial chemistry of each 300 pound heat was poured into a 100 pound ingot and given a suffix "A" to the heat number (Table 1), then alloy additions were made to the remainder of the VIM heat. The second 100 pound ingot with the enriched chemistry was poured and given a suffix "B" to the heat number and then further alloy additions were made to the remainder of the heat. The third and last 100 pound ingot was poured and given the suffix "C." The ingot dimensions were 4 x 4 x ?22 inch. These ingots were hot rolled at USS Technical Center into 3/4 inch thick plates that were cut into ?12 inch long plates. The cut plates were shipped to DTRC.

Chemical analysis of the plates produced by USS Technical Center are shown in Table 2. All the heats were low-carbon ranging from 0.012 to 0.029 wt. %. The low carbon levels were chosen to minimize the martensitic hardenability (Leslie, 1981). The purpose of the manganese, molybdenum, niobium, and

chromium additions was to reduce the temperature of bainite formation that thus increases the strength (Pickering, 1977). The nickel additions were to affect hardenability and low temperature (cleavage) toughness. The aluminum, phosphorous, sulfur, nitrogen, oxygen, and silicon levels in the steel were to reflect the levels of current full scale steel making practice. The small titanium additions were made to produce a fine distribution of TiN inclusions that removes free nitrogen from the matrix and may improve microstructural refinement of the grain size (Tanaka et al., 1975).

EXPERIMENTAL PROCEDURE

The experimental materials described above and listed in Table 2 were used to measure the effects of various alloying elements on the strength and cooling rate sensitivity of low-carbon steel. The 3/4 inch thick plates of steel were subjected to autogenous gas-tungsten-arc welding (GTAW) in order to form a weld bead in the plate. This technique of forming an "as-deposited" weld bead eliminated the need to produce welding wire required for bead-on-plate studies. The autogenous GTAW process also minimized any changes in chemical composition of the steel between the base plate and the weld bead since a non-oxidizing argon-helium cover gas was employed. All welding was performed in the flat position. All materials, except 8033, were welded using two heat inputs of 60 and 120 kJ/in. The material 8033 was welded with heat inputs of 25, 35, 45, 55, 60, 80, 100, and 120 kJ/in. The purpose of the variation in heat inputs was to vary the cooling rate experienced by the weld pool region of the plate. The cooling rates were measured using thermocouples that were plunged into the weld pool behind the GTAW arc during the weld pass.

The welded plates were sectioned and machined into flat tensile specimen blanks. Some tensile blanks were then thermally cycled with a "Gleeble 1500" to simulate multi-pass welding. The "Gleeble 1500" thermal simulator heats the specimens by passing a large AC electrical current through the specimen blank to produce resistance heating. The current is

varied with time to reproduce the temperature versus time profile created in the heat-affect-zone (HAZ) of a weldment. Single, double, or triple thermal cycles were applied to the specimens. Single thermal cycles simulated the temperatures experienced in the coarse grained HAZ of a 3/4 inch thick plate with a heat input equal to that of the original autogenous GTAW weld. This thermal cycle had a peak temperature of about 2500#F. The second thermal cycle produced a peak temperature in the "inter-critical" temperature range approximately 1400#F; and the third cycle produced a peak temperature of approximately 1200#F that was in the "sub-critical" temperature range. The cooling rates associated with each of the thermal cycles were calculated using Gleeble 1500 software to be representative of the HAZ cooling rate for the original autogenous TIG weld pass in 3/4 inch plate.

The "Gleeble 1500" thermal simulator heats the specimen to the desired control temperature by applying a large 60 cycle alternating current through the specimen which causes resistance heating of the sample which in this case is a flat tensile specimen blank (approximately 1/8 x 1/2 x 3-4 inch). The resistance heating of such a bar is accomplished by clamping the ends of the bar in conductive metal grips that are used to apply the current. The grips are water cooled via internal passages. The use of relatively low frequency AC current to heat the specimen provides uniform resistance heating through the cross section of the sample and along its length, assuming constant material resistivity. However, since the grips of the thermal simulator are water cooled the resistance heating near the specimen ends cannot overcome the thermal conduction losses to the grips. This condition leads to the fact that unclamped region of a specimen in a "Gleeble" thermal simulator has a non-uniform temperature profile which is highest in the center near the thermocouple and falls off near the grips. To mitigate this condition the grips were set at 3/4 inch apart to provide a heated region which was larger than the 1/2 inch gage length of the tensile specimen. The region of the tensile blank with the largest temperature

deviation was therefore outside the gage length of the tensile specimen.

All the blanks were then machined into flat tensile specimens as shown in Figure 1. The specimens from plates welded with less than 70 kJ/in. heat input were removed in the longitudinal orientation yielding an all weld metal sample. The plates welded with greater than 70 kJ/in. heat input produced weld beads large enough to accommodate tensile specimens with transverse orientation with the weld metal encompassing the full gage length. All the tensile specimens were tested using a Tinius Olsen screw driven universal testing machine with a 60,000 pound capacity. The test data acquired during the tensile testing included load, stroke, extension from a 0.5 inch gage length extensometer, and in some cases strain from strain gages on the test specimen gage length. The data from the transducer signal conditioners were digitally recorded along with an analog plot of load versus extension. The data was analyzed to determine the 0.2% offset yield strength, ultimate tensile strength, and elongation to failure. The tensile tests were performed in accordance with ASTM E8. The specimen gage length to width ratio was 4 or greater.

RESULTS and DISCUSSION

The results of the tensile tests performed on the autogenous welds of ULCB steels are shown in Table 3 for the material in the as welded condition. The tensile results for weld metal that had experienced additional thermal cycles to simulate multi-pass welding are shown in Table 4. The measured 0.2% offset yield strengths ranged from 86 to 135 ksi. The ultimate tensile strengths ranged from 108 to 149 ksi with elongation to failure values of 12 to 23%.

The chemistries tested were originally selected using Equation 1, which predicts the strength of bainitic steel from the chemistry of the plate (Garcia, 1991).

$$\mathrm{YS\ (MPa)} = 25 * [\ 10.2 + 68.1*(C+N) + 1623*B + 46.3*(Ti+Nb) + 4.8*Mo + 2.6*Cr + 0.3*Ni\ ] + 116*(\text{grain size})^{1/2} \quad \text{in weight percent} \qquad \text{Eq. 1}$$

The chemistries were chosen to produce yield strengths of 100 to 145 ksi. Although the equation adequately predicted the strength at the lower values near 100 ksi, the equation over-predicted the strengths produced in the more highly alloy bainitic steel by approximately 15 ksi as shown in Figure 2. This would indicate that some coefficients in the linear equation used are not correct when extrapolated to higher values. The grain size term in the Equation 1 was ignored since grain size measurements were not performed. An austenite grain size of 50 micrometers would produce a strength addition of less than 4 ksi. The Garcia equation was developed for plate that had received significant thermo-mechanical processing (TMP) that was not explicitly factored into the equation. Since TMP cannot be applied to weld metal, the loss of the effect of TMP on strength was not calculated. This may account for some of the under-prediction of strength in the equation.

Figure 3 is a plot of the measured ultimate tensile strengths (UTS) of the ULCB weld metals versus the UTS values predicted by Equation 2 published by Heuschkel [1964] for high strength steel weld metals. Here again the equation from previous work over predicts the measured strength of these ULCB weld metals. The work by Heuschkel was concerned with martensitic microstructures that obtain significant strengthening from carbon.

$$\begin{aligned}\text{Ultimate Tensile} &= 43 + 200*N + 128*C + 73*V + 19.5*Mo + 17*Mn \\ \text{Strength, in ksi} &\quad + 15*Si + 13.5*Cr + 4.3*Ni \qquad \text{Eq. 2)}\end{aligned}$$

Although the strengths measured for these model ULCB steels were below those predicted from published equations, the range of strengths and ductilities indicated that there is a significant potential for such weld metals with yield strength of at least 130 ksi. This is well into the strength range of traditional martensitic steels. Although the data does not

indicate an upper strength limit, the results provide a good basis for continuation of research into these steels provided a minimal cooling rate sensitivity still exists at such strength levels.

Cooling Rate Sensitivity

The first heat of ULCB steel that was evaluated was material 8033. This material differed from the other steels due to its intentionally low yield strength of approximately 100 ksi. The material was the result of an earlier research program to develop a 100 ksi yield strength ultra-low-carbon bainitic ULCB plate steel. This steel was available for immediate evaluation at the beginning of the ULCB weld metal program. The autogenous gas-tungsten-arc welding (GTAW) of this plate was performed over the wide range of heat inputs of 25 to 120 kJ/in. Heat inputs were evaluated from 25 to 120 kJ/in. and were selected to encompass the cooling rates that were comparable to the cooling rates in gas metal-arc welding (GMAW) of HY-130 steel with heat input of 35 to 100 kJ/in. The results of the tensile tests performed on the autogenous welds of ULCB 8033 are shown in Figure 4. The average yield strengths for the applied heat input ranges varied from a low of 89 ksi at 120 kJ/in. to a high of 100 ksi for the autogenous ULCB welds produced with a heat input of 35 kJ/in. A smaller change in the average measured ultimate tensile strength of 7 ksi was observed over the same range of heat inputs. Although this material displayed an 11 ksi change in yield strength, this was less than 1/3 the change in yield strength measured in a series of multi-pass gas-metal-arc welds (GMAW) using a commercial alloy wire (120S) over a similar range of heat input values. Figure 5 displays the same measured strength of ULCB 8033 as in Figure 4 but as a function of the measured cooling rate at 1000^{O}F. The change in average yield strength at any cooling rate was 0.177 ksi/^{O}F/sec, and 0.112 ksi/^{O}F/sec for the ultimate tensile strength. The cooling rate was not measured for the GMAW 120S welds mentioned above, and therefore cannot be plotted, but the cooling rate sensitivity would be much

greater than that measured for this ULCB steel.

The ductilities of the as welded autogenous GTAW welds were measured with both percent tensile elongation and percent reduction in area. Both measurements displayed values in accordance with good ductility. The measured elongation varied from 13 to 23% as shown in Table 3. The reduction in area (%RA) varied from 57 to 67% as shown in Figure 6. The %RA appears to increase with increasing heat input. This effect is most likely due to the small reduction in strength as heat input increased.

Multi-Pass Simulation

The strength of single pass welds of carbon alloy steel is usually higher than that for a multi-pass weld of the same steel. The change in strength is the result of a "tempering" process that the bead receives from the thermal effects of the subsequent passes. This allows the carbon to come out of solution along with the dissolving of fine carbides, and form large carbides that do not contribute to strength. The effect of this process can be measured on the autogenous, single pass welds by using a "Gleeble" thermal simulator. The thermal simulator can apply a heating cycle or cycles to a tensile specimen blank that reproduces the temperatures experienced by a given weld bead as a result of the multi-pass welding process. Therefore, the second weld pass may produce a thermal cycle with a peak temperature of 2300 to 2800^{O}F. The third bead may produce a thermal cycle in the first bead with a peak temperature of 2000 to 2500^{O}F and so on. These effects can be modeled and reproduced for each applied heat input.

The effect of a single gleeble cycle on the measured strength of an as-welded autogenous GTAW for material 8033 is plotted in Figure 7. The single gleeble thermal cycles simulated a second bead applied with a heat inputs of 55 to 120 kJ/in. as plotted. The effect of this thermal cycle was not to reduce or "temper" the strength of the as welded material but to increase the strength of the 8033 ULCB steel. The increase in yield and ultimate tensile strength was small 3-5 ksi and

similar at all heat inputs. This increase in strength is probably due to a "secondary hardening" effect. The strong carbide formers, chromium, molybdenum and niobium, in this ULCB steel must precipitate as fine carbo-nitrides that contribute to strength via a dislocation pinning mechanism. Such a distribution of second phase particles would be too small to resolve in a transmission electron microscope for verification. However, the data of a small and uniform increase in strength as a result of a such a thermal cycle would be consistent with a large amount of precipitate former present, together with a small amount of carbon and nitrogen forming small and stable precipitates. Such precipitates would be stable and resistant of Oswald ripening. Some thermal strengthening in ultimate tensile strength (UTS) of 5 ksi or less was observed in 3 of the 5 steels evaluated with a single gleeble thermal cycle with heat input of 60 and 120 kJ/inch. These results are shown in Figures 8 and 9. The steels that did not display thermal hardening at either heat input rate (8026B + 8032C) had softening in UTS of less than 6 ksi. Changes in yield strength were similar to UTS.

An analysis to establish a significant linear relationship between the degree of thermal strengthening and the alloy composition was performed. Two apparent empirical relationships were found. A negative relationship between the amount of carbon and degree of thermal strengthening shown in Figure 10, and a negative relationship with the amount of manganese present, Figure 11. The negative relationship with carbon content is possible given that carbon is a stronger martensite former than a bainite former. However, this effect should have been offset by the formation of Nb(CN) precipitate in the re-heated microstructure. Since the carbon and nitrogen levels are low in these alloys, the niobium should tie-up all free interstitial carbon and nitrogen. Without any free C or N in the weld further hardening via the other less potent carbide formers (Cr, Mo) becomes difficult. The negative relationship between manganese and thermal hardening cannot be explained by the author.

The effect of subsequent second and third Gleeble thermal cycles on the strength of an as-welded autogenous GTAW of ULCB steel was investigated using materials 8032C and 8026C. Figure 12 presents the measured strength of material 8026C in the as-welded and Gleeble thermal cycled condition. Some as-welded tensile blanks received 2 thermal cycles and others received three cycles. The 2-cycle and 3-cycle Gleeble thermal hardening increase the strengths of the as-welded tensile specimens by a similar amount of 5 to 10 ksi at 60 kJ/in. The thermal hardening had the added benefit of further minimizing any cooling rate effect by equalizing the yield and tensile strengths at the 60 and 120 kJ/inch heat input. The 8026C materials experience slight thermal softening as a result of single and double Gleeble cycles as shown in Figure 13. Here again the thermal effect appears to have a slightly beneficial effect on cooling rate sensitivity. Therefore, thermal softening in these alloys may be slight and benign.

The phenomenon of thermal hardening in these alloys may be beneficial for three reasons. First, the alloy strengthening occurs without added alloy or increased processing (free strengthening). Second, the strengthening may help resolve some of the discrepancies between the strengths measured and those predicted by published models. Thirdly, and most importantly, a thermal hardening process during multi-pass welding may provide a greater resistance to hydrogen cracking. The concept of a weld bead becoming stronger as the result of additional thermal cycles also means that the same weld bead would have a greater chance of a reduction in its hydrogen level. The thermal cycles that increase strength produce the thermal activity to allow greater time for hydrogen out-gassing. This is unlike the normal scenario for higher carbon steel that are most vulnerable to hydrogen (high as-deposited hardness) when the hydrogen level is greatest.

Effects of Alloying on Strength

The model ULCB steel chemical compositions were chosen to provide a matrix of alloys that could be used to isolate the

effects of the alloying elements; molybdenum, manganese, nickel, niobium, and carbon. A measure of the effectiveness of one of these alloying elements can be calculated by comparing the strengths of a pair of alloys that have similar chemistries except for the elements of interest. For example, alloys 8032B and 8032C have very similar chemistries, except for their manganese levels which are 1.47 and 1.96 wt.%. The effectiveness of manganese in such an alloy can be seen by plotting the measured strengths of the two alloys versus wt. % manganese for the two GTAW heat inputs investigated as shown in Figure 14. Plotted in Figure 14 are the measured yield and ultimate tensile strengths for 8032B and 8032C as-welded GTAW welds with 60 and 120 kJ/in heat input versus wt. % of manganese.

The lines in the figure are drawn between the average value of similar sets of tensile data such as yield strengths at 60 kJ/in. for the two different manganese level alloys. The absolute strength levels of the lines are a reflection of the total alloying, not just the one element of interest. The slope of the lines is a measure of the relative strengthening or hardening of manganese in these ULCB steels. The difference between the two yield strength or ultimate tensile strength lines is a measure of the cooling rate sensitivity of the alloy. From Figure 14 it can be observed that these alloys have yield strengths of approximately 120 and 130 ksi with a small amount of cooling rate sensitivity (about 5 ksi). Also apparent is the positive slopes of all the lines indicating that additional manganese has contributed to additional strength in these alloys. Since all the lines are approximately parallel, it appears that manganese does not affect the relative cooling rate sensitivity of these alloys. The slope of these lines (ksi/wt.%) is a measure of the effectiveness of manganese as hardening element. The slope of the two yield strength lines are 22.5 and 18.4 ksi/wt.% for the 60 and 120 kJ/in. heat input, respectively. These values are also listed in Table 5 under the column titled ">1.5 wt. % Mn" since the data covers the range of 1.5 - 2 wt.% Mn. The

data is in the row marked 1.4-2.4-3.4 (Mn-Mo-Ni) that is the nominal composition of the alloys, exclusive of the alloying element of interest.

Figures 15 through 25 are similar to Figure 14 but concern other alloying elements (Mo, Ni, Nb, and carbon) in different matrix combinations. Table 5 contains a summary of the data shown in Figures 14 through 25 for all the combinations of materials investigated. Also listed in Table 5 are the strength coefficients for the Heuschkel equation (Heuschkel, 1964) developed for high strength weld metal. An examination of Table 5 reveals some of the nature of alloy interactions in ULCB steels. The relative effectiveness of the alloying elements investigated is reflected by the order of the magnitude of the data listed. The element with the greatest slope is carbon followed by Nb then Mn and finally Mo and Ni (which were similar). This sequence differs from relative ranking of the coefficients of the Heuschkel equation also listed in Table 5 which ranked the effectiveness of the alloying elements carbon, Mo, Mn, and Ni (Nb was not investigated).

The ULCB data also demonstrates that the effectiveness of some alloying elements diminishes at high levels as the result of alloy interactions. For example, the measure of the effectiveness of nickel changes from a positive (with values of 6.2 and 5.3 ksi/wt.% up to 3.5%) to a negative (with values of -2.3 and -1.1 wt.%). This effect also occurs with manganese at the 1.5 wt.% level in alloys with 3.4 Mo - 3.4 Ni. The strengthening ability of the alloys often depends on the other alloys present. For example, the effectiveness of molybdenum is reduced as the Mn and Ni level is increased. The effectiveness of niobium for increasing strength is very strong in all the matrices investigated. In most cases the effect of alloying on the cooling rate sensitivity was small.

The average of the hardening potential of each alloy at the two GTAW heat inputs for each element is shown in Table 6. The coefficients derived from alloy-pairs are compared with the coefficient calculated from a linear regression analysis

performed on all the tensile data shown in Table 3. The linear regression data coefficient for manganese is reasonable compared to the coefficients derived from alloy-pairs as is the value for nickel when less than 3.5 wt.%. However, the linear regression analysis approach to such data cannot be used to identify alloy limits or levels of diminished returns or slope reversals as observed in this data.

This type of linear regression analysis is appropriate for comparison to published equations such as those listed in Table 6. The equations include the Heuschkel equation for high strength weld metals, the Pickering equation (Pickering, 1977) for higher carbon bainitic steel plate, and the Garcia equation (Garcia, 1991) for ULCB steel plate. It is not reasonable to expect that coefficients of different analyses to be numerically similar. However, these different numerical analyses performed on entirely different data sets should all reflect similar principles of physical metallurgy. The relative ranking of the coefficients of the alloying elements from all the equations should be similar. The rankings for the results of the analysis performed on these ULCB data and the other published equations are listed below in Table 7. The relative ranking of carbon, niobium and nickel appear similar in all four analyses. The relative position of manganese and molybdenum is not consistent. The current work and the Pickering work rank manganese more effective than molybdenum. This shows that the potency of some alloying element may change, possibly due to alloy interactions, as was indicated in Tables 5 and 6.

Table 7. Ranking of Coefficient Values in Published Equations

SOURCE	COEFFICIENT RANKING (Strong to Weak)
Current work	C, Nb, Mn, Mo, Ni
Heuschkel	C, Mo, Mn, Ni (did not evaluate Nb)
Pickering	C, Mn, Mo, Ni (did not evaluate Nb)
Garcia	C, Nb, Mo, Mn, Ni

The results described above suggest that some reasonable assessment of interaction coefficients should be included in any linear regression analysis of such a data set. Such an analysis was performed on the data that included as the primary chemistry data not only the listed C, Mn, Mo, Ni, and Nb as listed in Table 2, but also three extra columns of data which were the products of Mn * Mo, Ni * Mo, and Mn * Ni (wt. %). The resulting equation, which predicts the measured UTS, was as follows:

$$\text{U.T.S (ksi)} = (-84.7) + 316{*}C + 120{*}Mn + 63{*}Nb + 19.6{*}Mo - 8.66{*}(Mn{*}Mo) - 0.183{*}(Ni{*}Mo) - 22.9{*}(Mn{*}Ni) \quad \text{Eq.3)}$$

The analysis for this equation produced a R-squared value of 0.964 which was higher than the 0.85 value obtained for the previous analysis performed without the interaction coefficients. The values predicted by Equation 3 for the ULCB chemistries investigated are shown in Figure 26, plotted against the measured UTS values. Equation 3 appears to do a good job of describing the data and it shows that there are some negative interactions that occur with the alloying elements. These negative interactions were observed for molybdenum at high manganese levels and for manganese at high molybdenum levels, but the (Mn-Ni) combination was not investigated. Although the equation indicates that the Mn-Ni interaction is worse than the other two interactions, the numerical value should not be taken out of the context of this equation which has some doubtful physical significance since the intercept value of the equations is also negative. The physical significance of a negative intercept (which should represent the unalloyed strength of iron) is difficult to imagine. Another similar analysis performed on this data to predict the yield strength of the ULCB weld metals produced an equation with an extremely high intercept value of 318 ksi and negative coefficients for nearly all the other terms. This equation had a R-squared value of 0.922. Although the physical significance of many such

equations may not exist, they can be used to suggest that there are some negative interactions that are at work in this set of ULCB weld metal data. This would support the results of the analysis of alloy-pairs discussed above.

The above discussion has revealed two general relationships concerning the GTAW ULCB welds investigated;

a) The effects of changes in the level of alloying elements on the measured strengths of these welds does not appear to be a linear relationship.

b) Negative interactions were observed concerning the effects of alloying elements on measured strengthening potency. Considering these statements leads to two general statements about the data. First, it cannot be assumed that strength levels greater than those measured in these alloys are possible for ULCB weld metal. Second, that ULCB welds of the strengths measured in this work should be achievable with less alloying once the effects of the negative interaction are understood and optimized.

SUMMARY

The purpose of this investigation was to measure the effects of various alloy additions on the strength and cooling rate sensitivity of low-carbon weld metal (model materials). A series of ultra-low-carbon alloy steels were subjected to autogenous gas-tungsten-arc welding (GTAW) with a range of heat inputs. The welded metals were subjected to tensile tests. A summary of the results of this program is listed below.

The measured yield strengths of the as-welded model materials ranged from 92 to 135 ksi, with ultimate tensile strength from 108 to 149 ksi.

The cooling rate sensitivity of these steels was very small compared conventional weld metals.

The effect of simulated multi-pass welding on 4 of 5 alloys evaluated caused some increase in strength over the as-welded materials. The change in strength was less than $\pm$ 8 ksi for alloys evaluated.

The relative ranking of the strengthening potential of alloying elements C, Nb, Mn, Mo, and Ni appears generally similar to the relative ranking in published equations for high strength weld metal and bainitic steels.

Some alloying elements appear to have negative interaction coefficients with each other, which creates difficulties for the use of linear equations to describe the relationship between strength and alloy composition for the weld metals.

REFERENCES

Bain, E. C. and H. W. Paxton, Alloying Elements in Steels, American Society For Metals, Metals Park Ohio, 1966, pp. 242-243.

Dorschu, K. E. and A. Lesnewich, Welding Journal Research Supplement, Vol. 42, 1964, p. 97S.

Garcia, I., et al., "Ultra-Low Carbon Bainitic Plate Steels: Processing, Microstructure, and Properties," Transactions of ISS, Oct. 1991, pp. 97-107.

Heuschkel, J., "Composition Controlled, High-Strength, Ductile, Tough, Steel Weld Metal," Welding Research Supplement, pp. 361-384, August, 1964.

Leslie, W. C., The Physical Metallurgy of Steels, McGraw Hill Book Company, 1981, p. 251-252.

Linnert, G. E., Welding Metallurgy Volume 2, American Welding Society, Inc., New York, 1967, p. 142-145.

Pickering, F. B., Microalloying 75, Union Carbide Corp., New York, 1977, p. 9-31.

Tanaka, J. et al., Transactions of the Iron and Steel Institute of Japan, Vol. 15, 1975, p. 19-26.

Table 1. Target Chemistries for Model Weld Metals
Compositions in wt. %

Heat ID.	C	Mn	Mo	Ni	Nb	Si	Al	Ti	N
8025A	0.02	1.0	3.5	3.5	0.05	0.2	0.01	0.01	0.008
8025B	0.02	1.5	3.5	3.5	0.05	0.2	0.01	0.01	0.008
8025C	0.02	2.0	3.5	3.5	0.05	0.2	0.01	0.01	0.008
8026A	0.02	1.5	2.5	2.5	0.05	0.2	0.01	0.01	0.008
8026B	0.02	1.5	3.5	2.5	0.05	0.2	0.01	0.01	0.008
8026C	0.02	1.5	3.5	4.0	0.05	0.2	0.01	0.01	0.008
8027A	0.02	1.5	2.5	3.5	0.00	0.2	0.01	0.01	0.008
8027B	0.02	1.5	2.5	3.5	0.40	0.2	0.01	0.01	0.008
8027C	0.02	1.5	2.5	3.5	0.60	0.2	0.01	0.01	0.008
8028B	0.02	1.5	3.5	3.5	0.03	0.2	0.01	0.01	0.008
8028C	0.02	1.5	3.5	3.5	0.05	0.2	0.01	0.01	0.008
8029A	0.02	1.5	2.5	3.5	0.05	0.2	0.01	0.01	0.008
8029B	0.02	1.5	2.5	4.0	0.05	0.2	0.01	0.01	0.008
8029C	0.02	1.5	2.5	4.5	0.05	0.2	0.01	0.01	0.008
8032B	0.02	1.5	2.5	3.5	0.05	0.2	0.01	0.01	0.008
8032C	0.02	2.0	2.5	3.5	0.05	0.2	0.01	0.01	0.008
8033	0.02	1.0	1.7	3.5	0.05	0.2	0.01	0.01	0.008

Table 2. Chemical Compositions of Model Materials
Compositions in wt. %

Heat ID.	C	Mn	Mo	Ni	Nb	Cr	Si	Al	Ti	N
8025A	0.022	1.00	3.51	3.40	0.061	0.23	0.20	0.015	0.010	0.010
8025B	0.023	1.47	3.46	3.35	0.061	0.23	0.22	0.011	0.006	0.010
8025C	0.023	2.00	3.44	3.34	0.060	0.23	0.20	0.010	0.005	0.009
8026A	0.018	1.44	2.44	2.46	0.057	0.23	0.18	0.013	0.009	0.009
8026B	0.018	1.40	3.50	2.48	0.059	0.22	0.23	0.006	0.009	0.005
8026C	0.018	1.33	3.35	4.03	0.060	0.21	0.19	0.008	0.004	0.008
8027A	0.015	1.46	2.36	3.45	0.002	0.23	0.19	0.017	0.007	0.006
8027B	0.015	1.45	2.33	3.42	0.045	0.23	0.21	0.010	0.008	0.007
8027C	0.016	1.43	2.32	3.40	0.045	0.23	0.19	0.009	0.007	0.006
8028B	0.016	1.39	3.50	3.50	0.031	0.22	0.19	0.008	0.008	0.008
8028C	0.015	1.40	3.51	3.54	0.046	0.22	0.18	0.007	0.006	0.008
8029A	0.026	1.44	2.33	3.39	0.028	0.23	0.18	0.019	0.010	0.006
8029B	0.023	1.38	2.26	4.30	0.052	0.22	0.20	0.009	0.009	0.006
8029C	0.020	1.41	2.27	4.36	0.052	0.23	0.23	0.009	0.009	0.006
8032B	0.028	1.47	2.49	3.45	0.051	0.23	0.18	0.007	0.007	0.005
8032C	0.029	1.96	2.48	3.43	0.050	0.23	0.20	0.006	0.008	0.005
8033	0.012	0.99	1.75	3.50	0.050	0.30	0.20	0.013	0.012	0.007

Sulfur and Phosphorus each less than 0.005 wt. %

Table 3. Flat Tensile Specimen Test Results of As-Welded Autogenous GTAW

Heat-	Spec. ID.	Heat Input (kJ/in)	0.2% Yield Strength (ksi)	Ultimate Tensile (ksi)	Percent Elongation (%)
8025A	5A1	60	114	125	21
	5A2	60	114	132	20
	5A14	60	115	133	21
	5A3	120	113	127	16
	5A4	120	114	128	20
	5A5	120	113	130	21
8025B	5B17	60	125	139	20
	5B20	60	129	141	18
	5B21	60	132	141	18
	5B4	120	124	137	18
	5B5	120	125	136	19
	5B8	120	121	134	23
8025C	5C22	60	126	143	19
	5C23	60	130	149	18
	5C24	60	129	143	20
	5C3	120	126	140	19
	5C4	120	123	140	20
	5C5	120	123	136	20
8026A	6A15	60	111	129	20
	6A16	60	115	130	23
	6A17	60	112	128	20
	6A3	120	113	119	21
	6A4	120	107	120	22
	6A5	120	109	122	21
8026B	6b19	60	115	132	21
	6b20	60	121	134	21
	6b22	60	117	135	22
	6B7	120	114	126	20
	6B8	120	114	127	20
	6B9	120	118	130	20
8026C	6C19	60	125	134	17
	6C20	60	125	135	19
	6C21	60	126	138	20
	6C7	120	130	136	15
	6C8	120	133	145	12
	6C9	120	124	132	18
8027A	7A15	60	113	126	21
	7A17	60	118	128	21
	7A20	60	110	126	21
	7A3	120	113	126	19
	7A5	120	109	119	20
	7A6	120	111	122	20

Table 3. (Continued) Flat Tensile Specimen Test Results of As-Welded Autogenous GTAW

Heat-	Spec. ID.	Heat Input (kJ/in)	0.2% Yield Strength (ksi)	Ultimate Tensile (ksi)	Percent Elongation (%)
8027B	7B17	60	115	123	21
	7B18	60	119	126	21
	7B19	60	124	124	21
	7B4	120	115	126	20
	7B5	120	114	122	22
	7B7	120	114	123	21
8027C	7C19	60	116	127	21
	7C20	60	115	125	21
	7C21	60	111	124	19
	7C3	120	126	122	19
	7C4	120	111	121	21
	7C6	120	118	123	20
8028B	8b15	60	120	133	20
	8b16	60	118	131	19
	8b17	60	117	133	19
	8b3	120	117	126	20
	8b4	120	118	129	19
	8b5	120	115	126	21
8028C	8C19	60	122	132	21
	8C20	60	123	134	19
	8C21	60	123	136	20
	8C3	120	116	127	20
	8C4	120	119	129	19
	8C5	120	119	130	20
8029A	9A18	60	114	126	21
	9A19	60	116	131	22
	9A21	60	113	130	22
	9A3	120	112	126	20
	9A4	120	112	124	22
	9A5	120	108	123	22
8029B	9B1	60	113	128	20
	9B2	60	118	128	21
	9B14	60	119	130	15
	9B3	120	114	120	22
	9B5	120	112	126	22
	9B6	120	112	126	22
8029C	9C1	60	118	135	20
	9C2	60	125	141	19
	9C3	120	113	129	21
	9C4	120	119	128	20
	9C5	120	114	129	20

Table 3. (Continued) Flat Tensile Specimen Test Results of As-Welded Autogenous GTAW

Heat-	Spec. ID.	Heat Input (kJ/in)	0.2% Yield Strength (ksi)	Ultimate Tensile (ksi)	Percent Elongation (%)
8032B	2B17	60	123	135	21
	2B18	60	121	134	20
	2B19	60	117	131	21
	2B3	120	117	126	18
	2B5	120	117	127	19
	2B6	120	116	126	22
8032C	2c22	60	135	149	21
	2c23	60	128	144	19
	2c7	120	124	136	20
	2c8	120	131	143	17
	2c9	120	122	136	20
8033	3a1	25	105	122	15
	3a2	25	103	123	21
	3a3	35	100	119	13
	3a4	35	102	117	17
	3a5	45	101	117	16
	3a6	45	93	108	16
8033	3a7	55	92	115	14
	3a8	55	94	123	13
	3a9	55	98	115	16
	3a10	60	94	114	12
	3a11	60	95	117	16
	3a12	60	94	113	15
	3a13	60	96	112	14
8033	3a14	80	92	115	22
	3a15	80	94	115	20
	3a16	80	95	115	21
	3a17	80	95	115	22
	3a18	100	91	113	22
	3a19	100	93	112	21
	3a20	100	93	108	21
	3a21	100	93	113	22
	3a22	120	91	110	23
	3a23	120	89	109	23
	3a24	120	86	111	21
	3a25	120	93	111	22

Table 4. Flat Tensile Specimen Test Results for Gleebled Specimens

Heat- Specimen ID.		0.2% Yield Strength (Ksi)	Ultimate Tensile (Ksi)	Percent Elongation (%)	Number and Heat Input of Simulated Thermal Cycle # - kJ/in.
8026B	6b18	120	136	22	1 - 60
	6b21	119	133	19	1 - 60
	6b3	115	127	20	1 - 120
	6b4	115	127	21	1 - 120
	6b5	118	131	21	SR*
	6b6	117	132	22	SR*
8026C	6c24	129	139	19	1 - 60
	6c23	131	137	19	1 - 60
	6c1	129	140	20	1 - 60
	6c18	125	138	21	2 - 60
	6c15	128	140	22	3 - 60
	6c16	125	136	21	3 - 60
	6c11	135	137	19	1 - 120
	6c6	125	136	18	2 - 120
	6c3	128	137	19	3 - 120
	6c4	127	136	20	3 - 120
8029B	9b18	120	134	20	1 - 60
	9b19	115	129	17	1 - 60
	9b8	117	129	19	1 - 120
	9b9	115	128	21	1 - 120
8032C	2c18	123	144	20	1 - 60
	2c21	117	132	20	1 - 60
	2c19	126	141	20	2 - 60
	2c20	127	142	21	2 - 60
	2c3	123	136	19	1 - 120
	2c4	122	135	12	1 - 120
	2c5	119	139	21	2 - 120
	2c6	123	139	20	2 - 120
8033	F55	102	112	20	1 - 55
	G55	95	119	18	1 - 55
	G60	104	118	19	1 - 60
	F80	95	119	19	1 - 80
	E100	92	113	21	1 - 100
	F100	97	117	19	1 - 100
	E120	92	113	22	1 - 120
	F120	97	110	22	1 - 120

SR* = Stress Relief of 1200F for 1 hour

Table 5. Change in yield strength (ksi) per wt.% alloying for ULCB steel for 60 and 120 kJ/inch heat input.

	ALLOYING ELEMENT / Heat Input (kJ/in.)															
Nominal	< 3.5 Ni		>3.5 Ni		Moly.		Carbon		<1.5 Mn		>1.5 Mn		<0.05 Nb		>0.05 Nb	
Composition	60	120	60	120	60	120	60	120	60	120	60	120	60	120	60	120
Mn–Mo–Ni	ksi/wt%		ksi/wt%		ksi/wt%		ksi/wt%		ksi/wt%		ksi/wt%		ksi/wt%		ksi/wt%	
1.4–2.4–3.4	6.2	4.2	–2.	–1.	––	––	76.	230	–––	–––	22.	18.	261	130	––	––
1.4–3.4–3.4	4.5	9.0	––	––	––	––	875	625	30.	21.	1.3	–1.	267	133	467	333
1.4–3.5–2.5	––	––	––	––	4.7	4.7	––	––	––	––	––	––	––	––	––	––
1.4–2.3–3.5	––	––	––	––	–1.0	2.0	––	––	––	––	––	––	140	70	––	––
2.0–2.3–3.4 in wt. %	––	––	––	––	–3.1	–2.1	––	––	––	––	––	––	––	––	––	––
							Published Equation									
Heuschkel	3.9	3.9	3.9	3.9	17.	17.	115	115	15.	15.	15.	15.	––	––	––	––

––– = not available or not measured;
Heushkel 1964, assumed delta UTS x (0.9) = delta YS

Table 6. Avarage change in yield strength (ksi) per wt.% alloying for ULCB steel.

Nominal	ALLOYING ELEMENT in wt. %							
Composition	<3.5 Ni	>3.5 Ni	Moly.	Carbon	<1.5 Mn	>1.5 Mn	<.05 Nb	>0.05 Nb
Mn–Mo–Ni	ksi/Wt.%	ksi/Wt.%	ksi/Wt.%	ksi/Wt.%	ksi/Wt.%	ksi/Wt.%	ksi/Wt.%	ksi/Wt.%
1.4–2.4–3.4	5.2	−1.7	---	153.5	---	20.5	195.5	---
1.4–3.4–3.4	6.75	---	---	750	25.95	0	200	400
1.4–3.5–2.5	---	---	4.7	---	---	---	---	---
1.4–2.3–3.5	---	---	0.5	---	---	---	105	---
2.0–2.3–3.4	---	---	−2.6	---	---	---	---	---
Linear Regression of Data	4.7	4.7	5.8	39.4	17.8	17.8	83.2	83.2
			Published Equations					
Heuschkel	3.9	3.9	17.6	115	15.3	15.3	---	---
Pickering	16.1	16.1	24.1	251	30.1	30.1	---	---
Garcia	1.1	1.1	17.4	247	12	12	168	168

--- = not available or not measured;

Heushkel 1964, assumed delta UTS x (0.9) = delta YS

Pickering 1975, assumed delta UTS x (0.9) = delta YS

Garcia, 1991

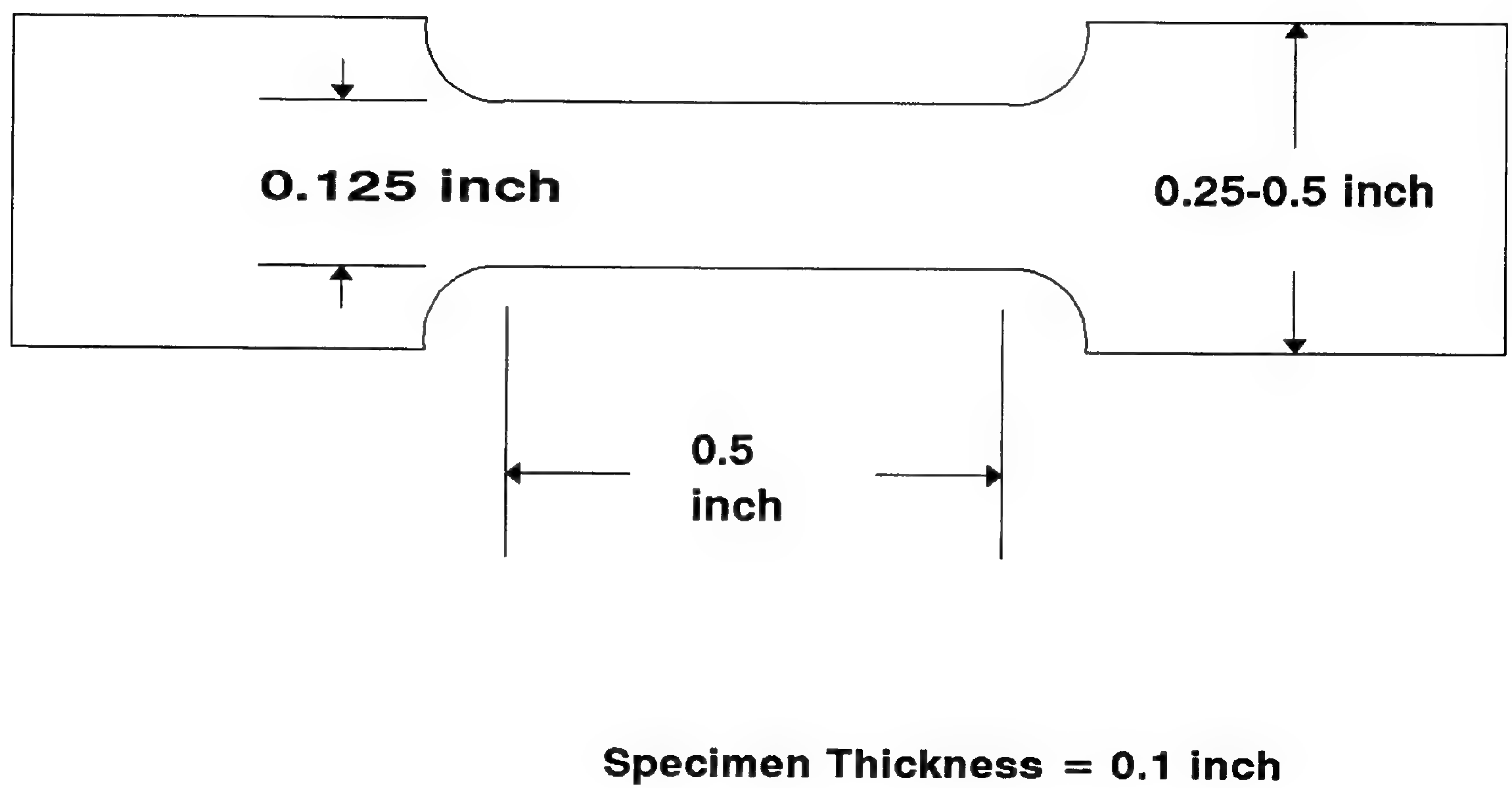

Figure 1. Sketch of flat tensile specimen.

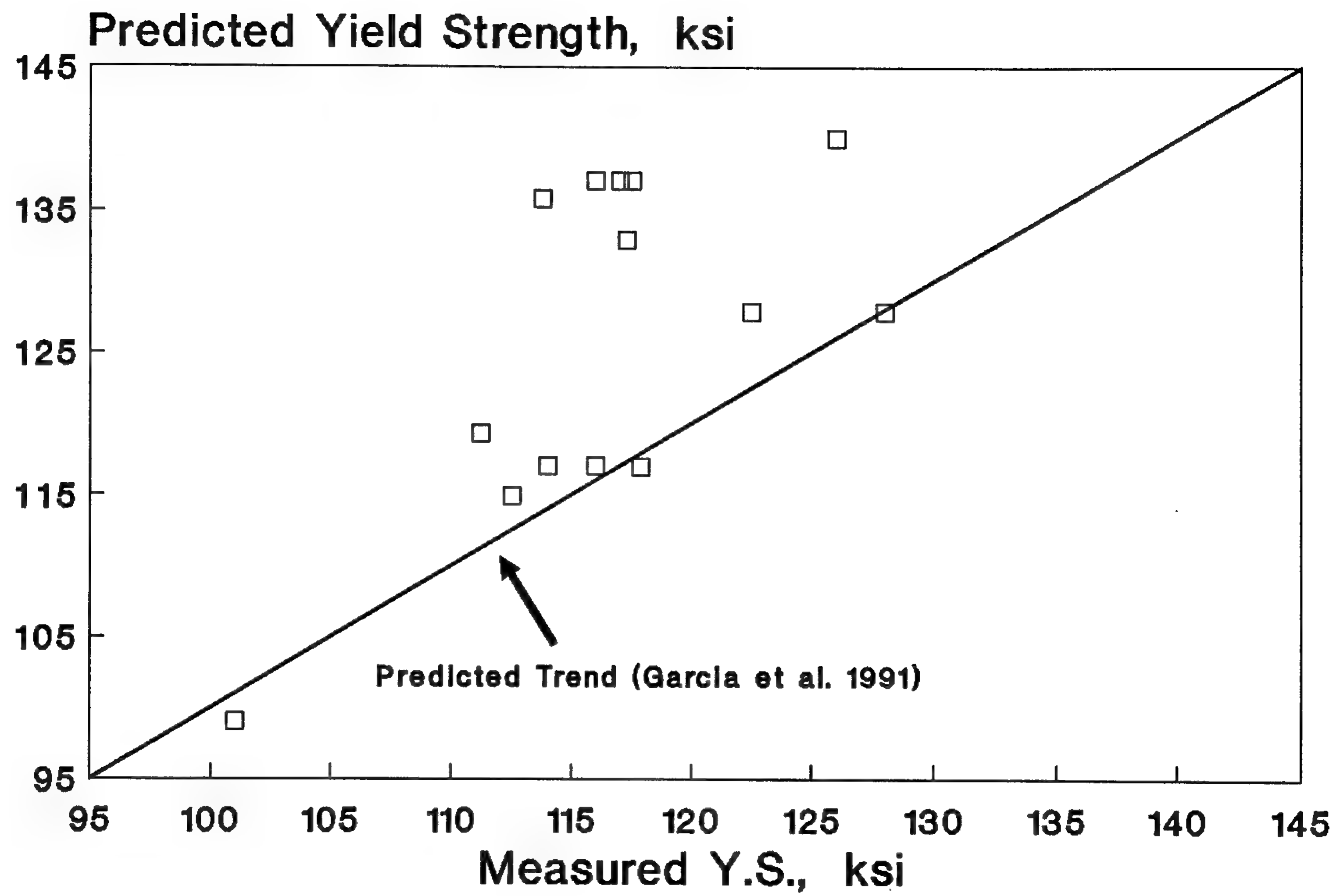

Figure 2. Measured versus prediddcted yield strength for ULCB steel welds using equation by Garcia (1991).

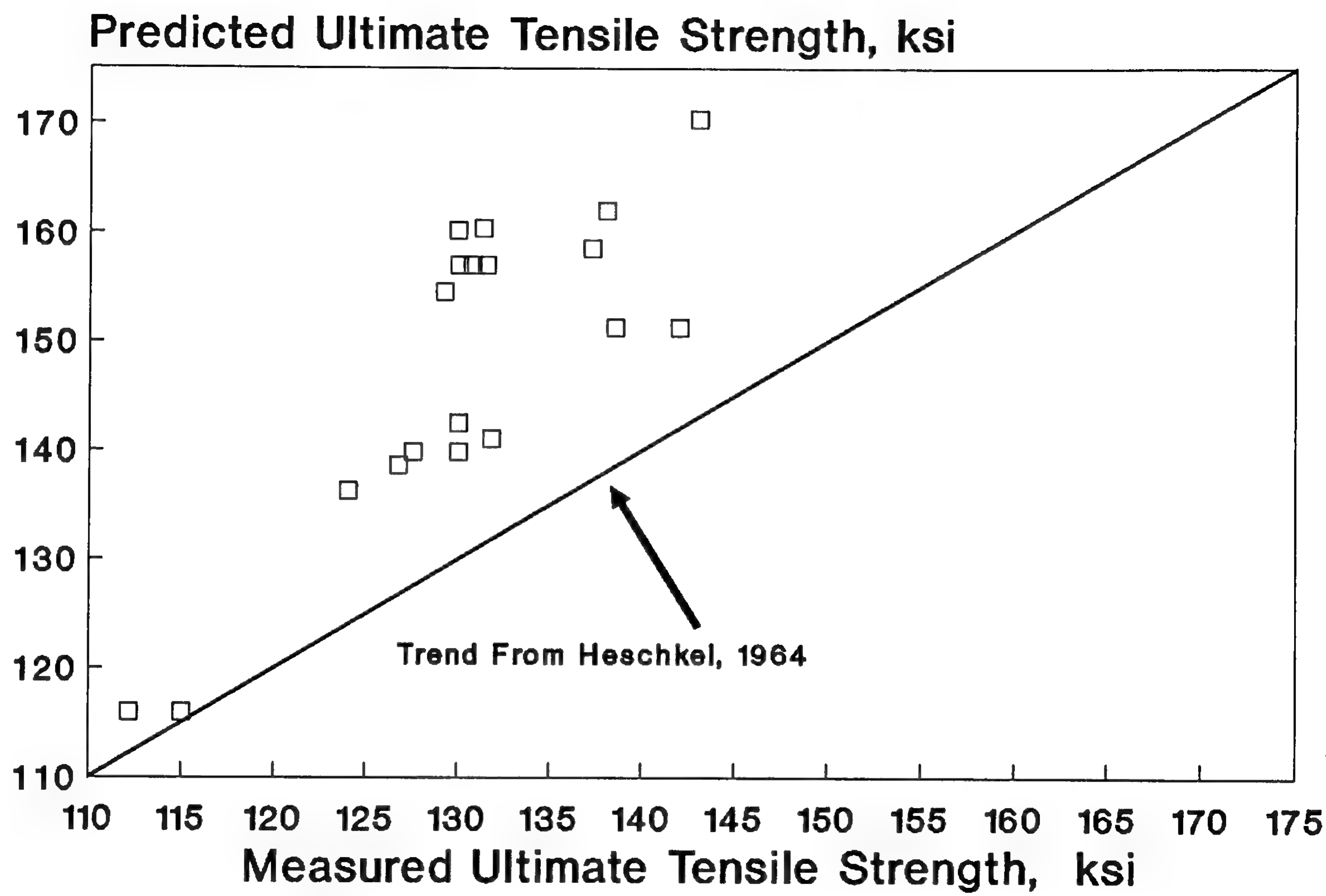

Figure 3. Measured versus predicted ultimate tensile strength for ULCB steel welds using Heschkel equation (1964).

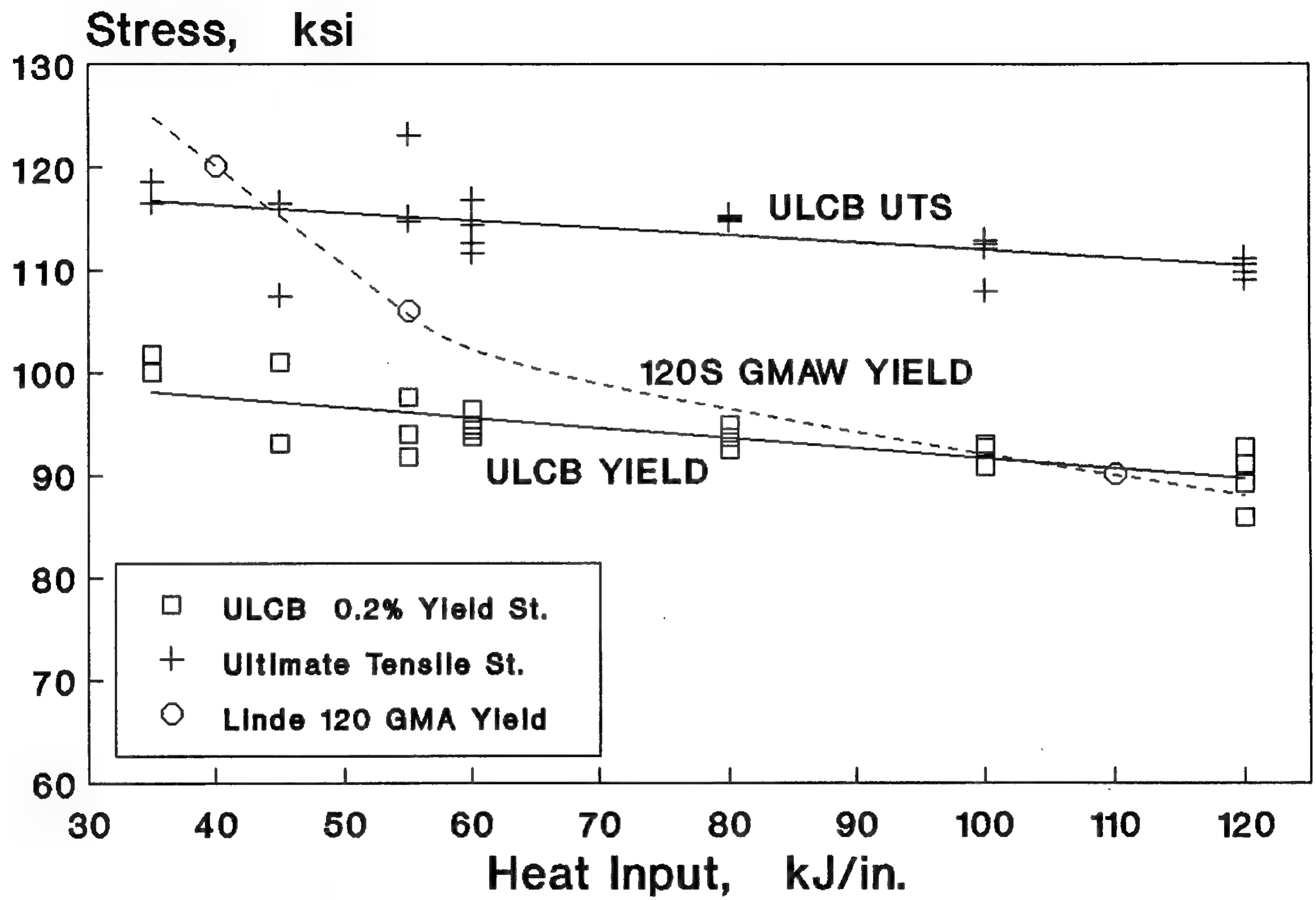

Figure 4. Measured yield and ultimate tensile strength for material 8033 vs. autogenous GTAW heat input.

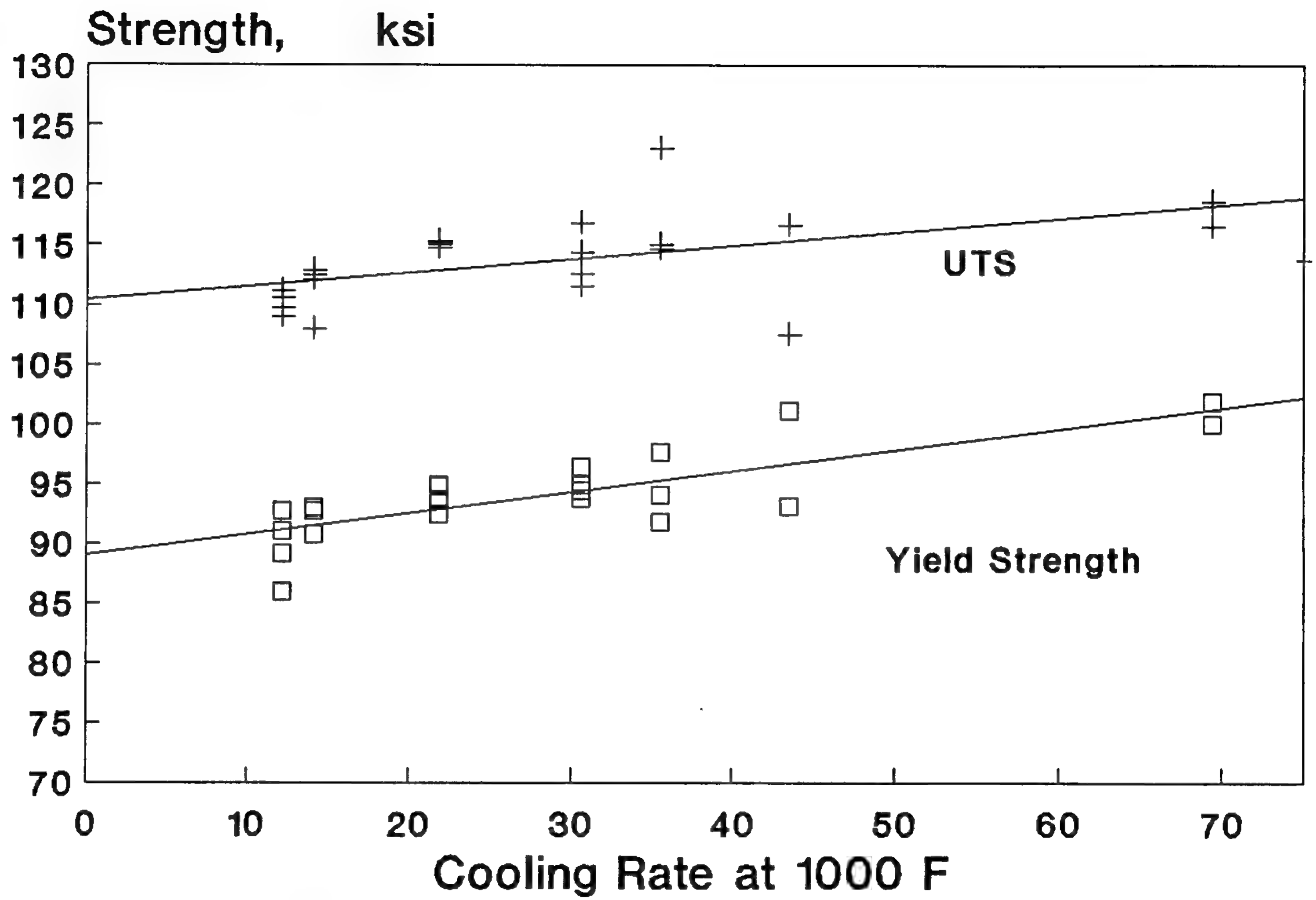

Figure 5. Measured Yield and Ultimate Tensile Strenght for ULCB 8033 versus Measured Cooling Rate at 1000F.

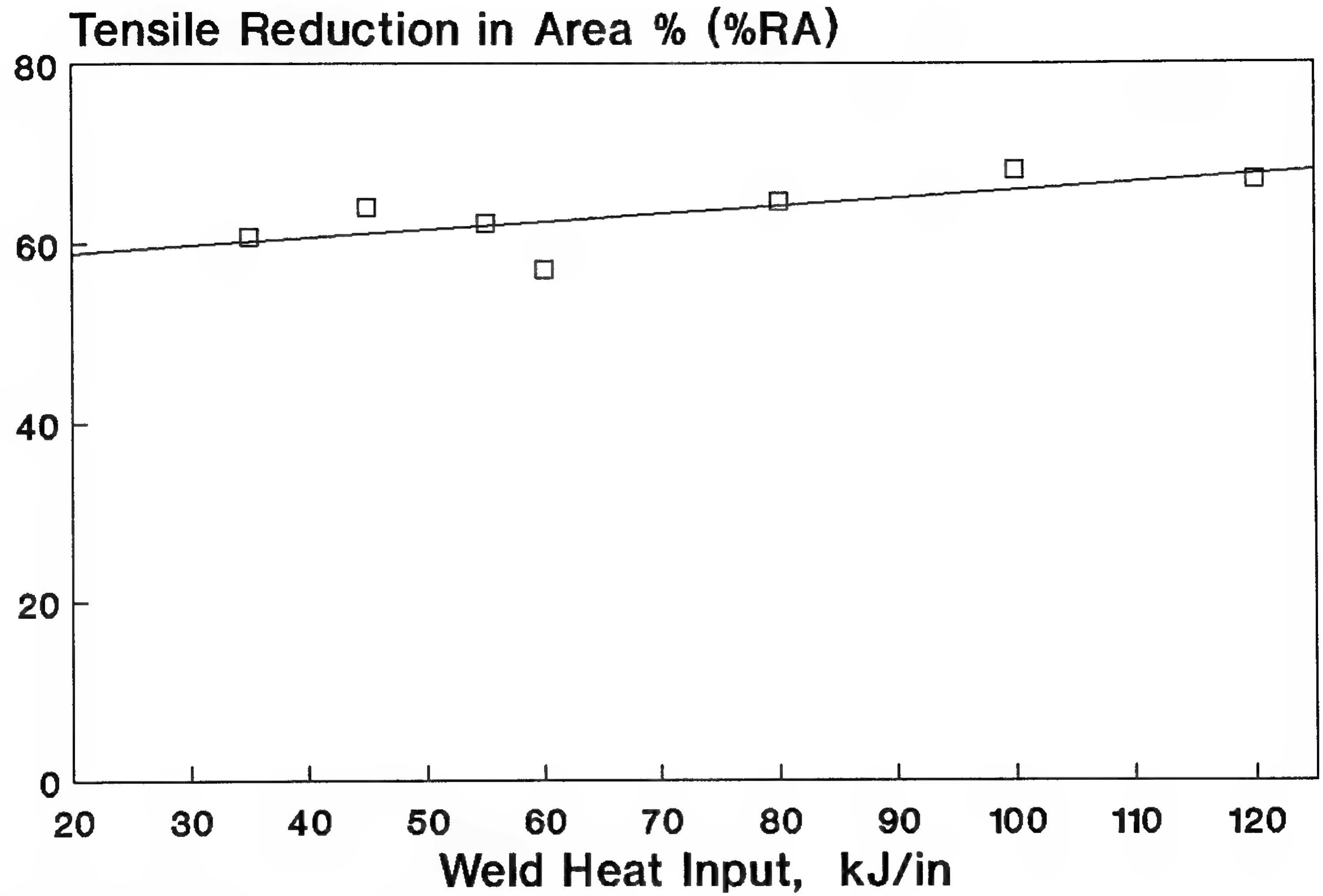

Figure 6. Percent reduction in area (%RA) for material 8033 versus autogenous GTAW heat input.

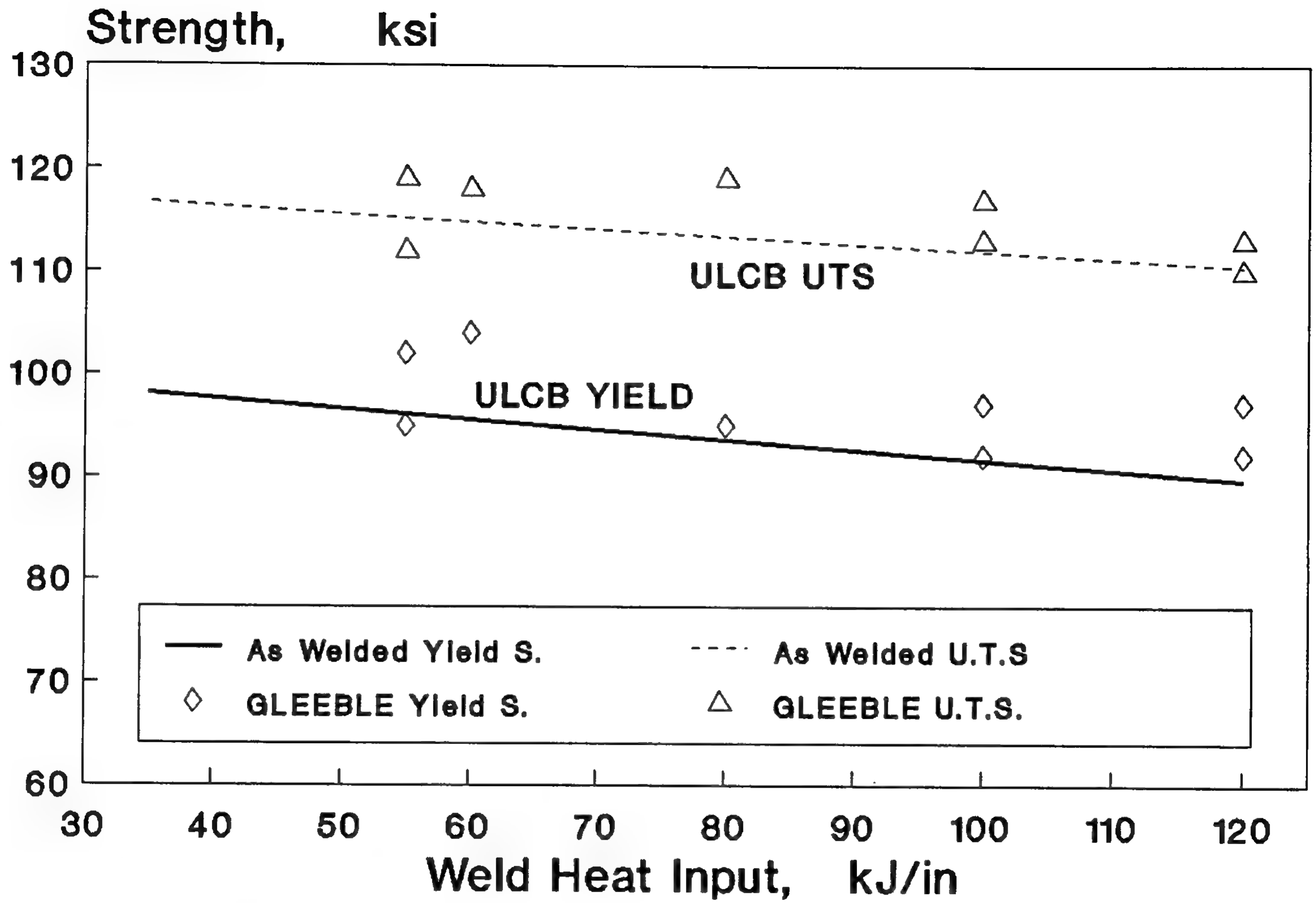

Figure 7. Effect of simulated multi
-pass welding on autogenous GTAW
weld properties of ULCB steel, 8033.

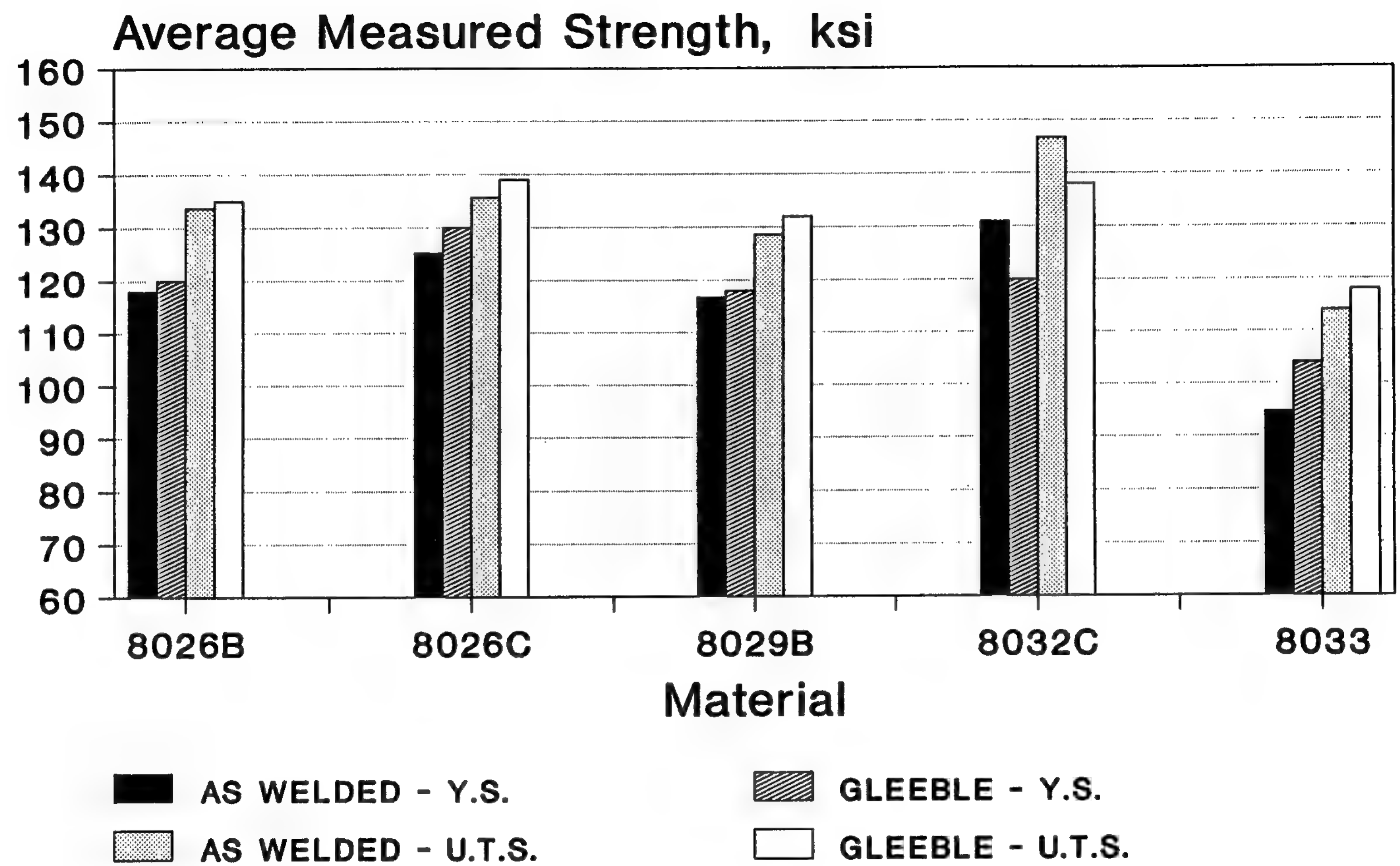

Figure 8. Effect of single Gleeble thermal cycle on the strength of as-welded ULCB metal GTAW at 60kJ/inch.

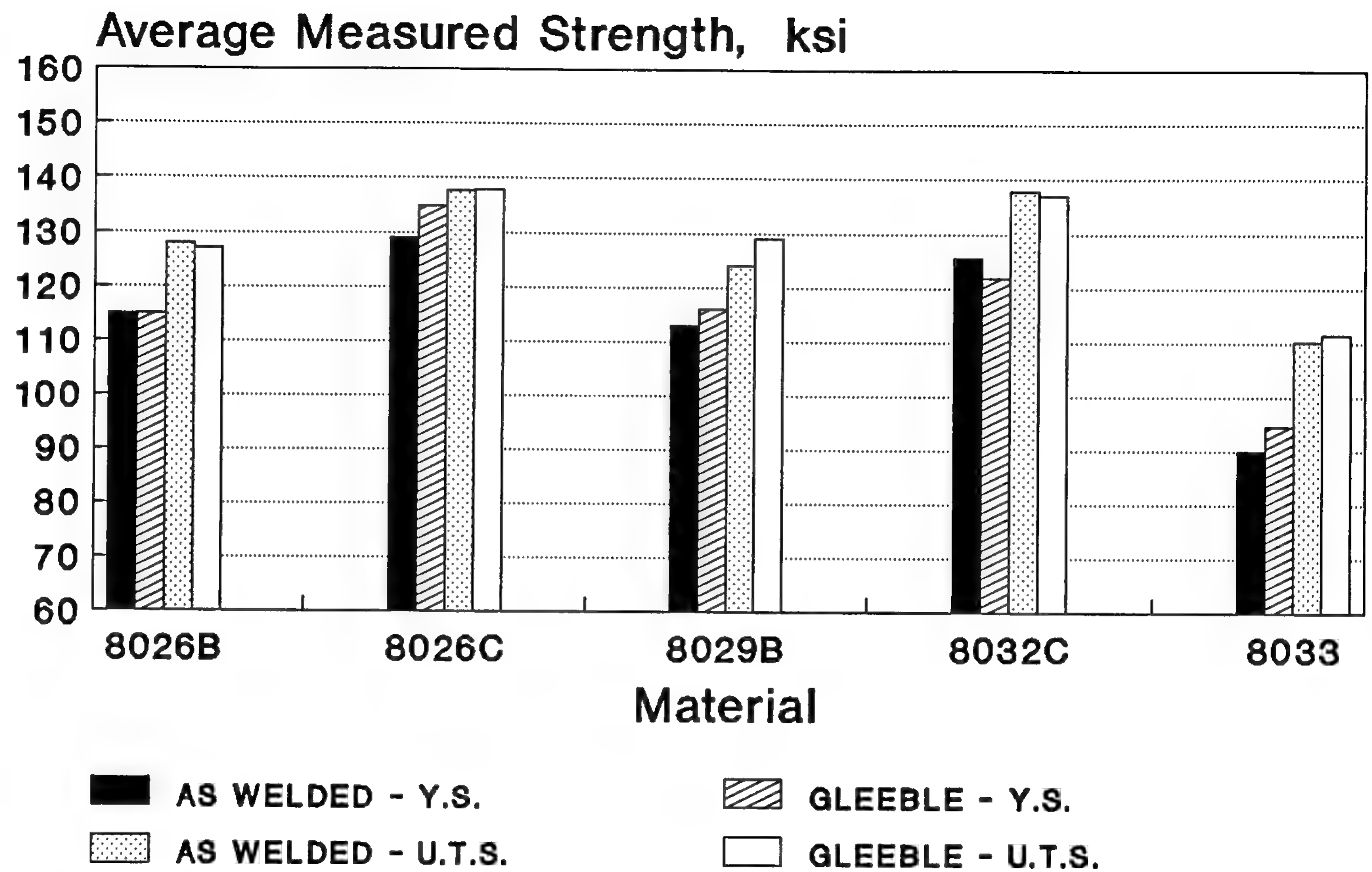

Figure 9. Effect of single Gleeble thermal cycle on the strength of as-welded ULCB metal, GTAW at 120 kJ/inch.

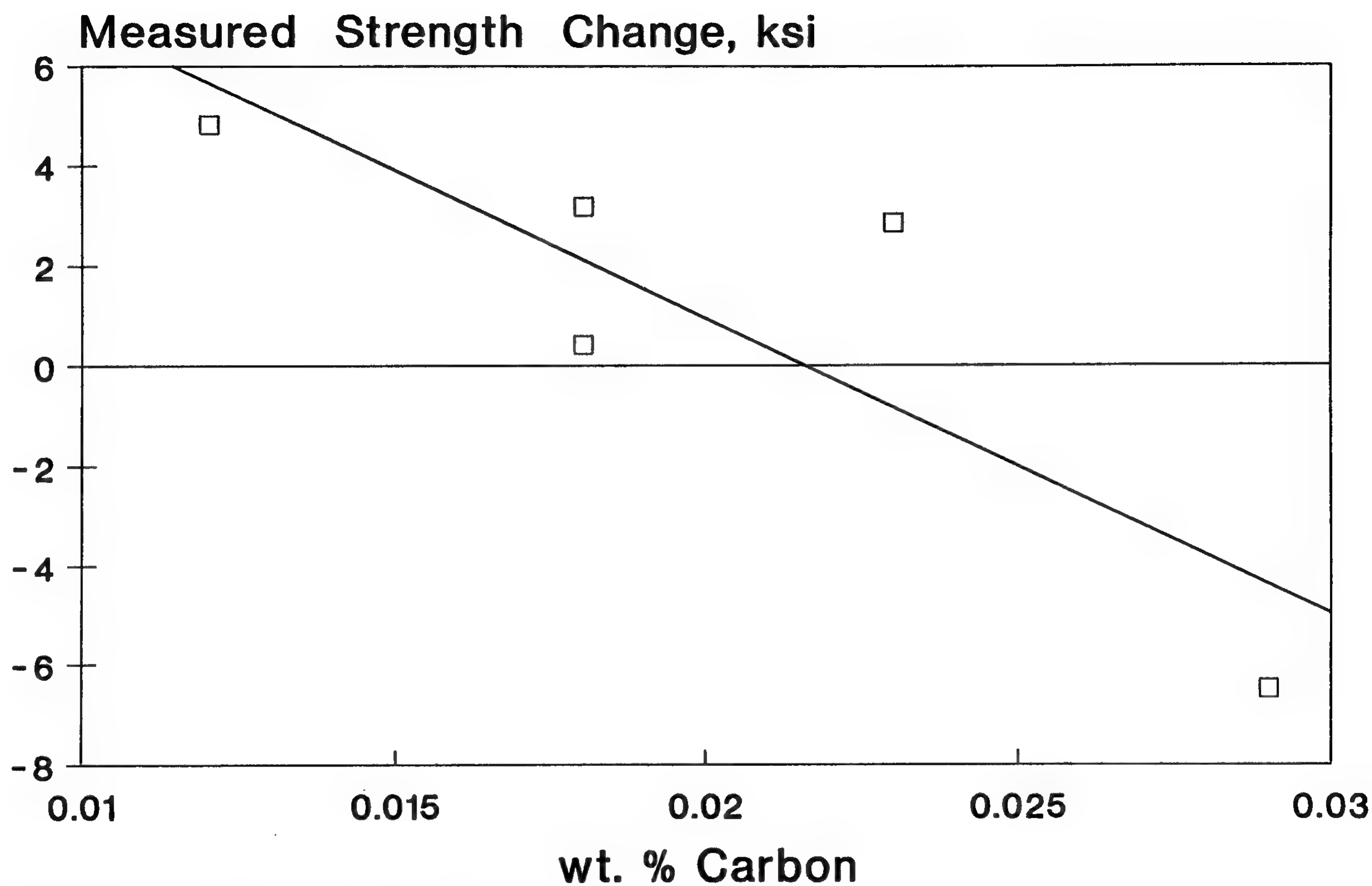

Figure 10. Change in measured yield and UTS strength of ULCB GTAW from Gleeble thermal cycle vs. carbon content.

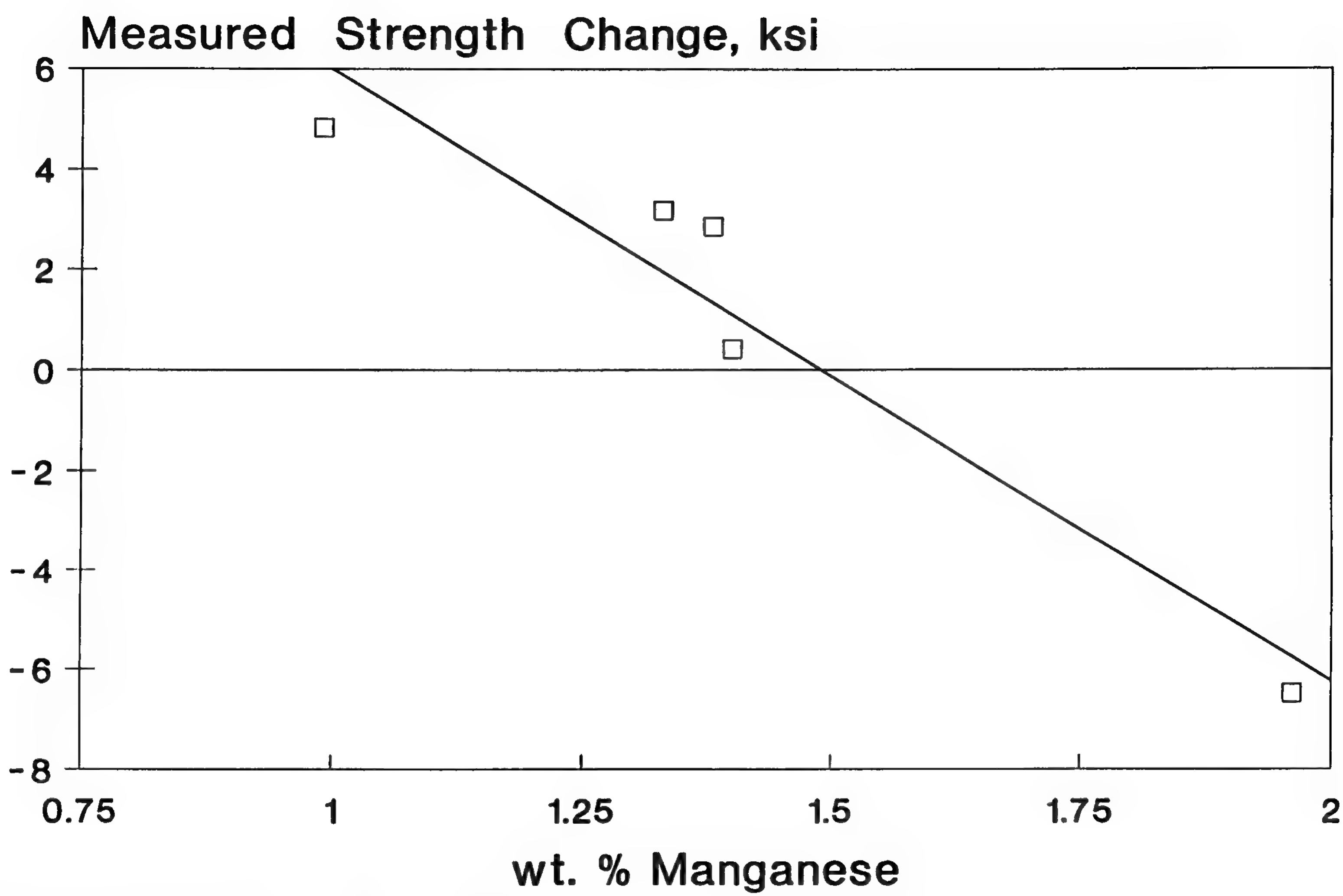

Figure 11. Change in measured yield and UTS strength of ULCB GTAW from Gleeble thermal cycle vs. manganese content.

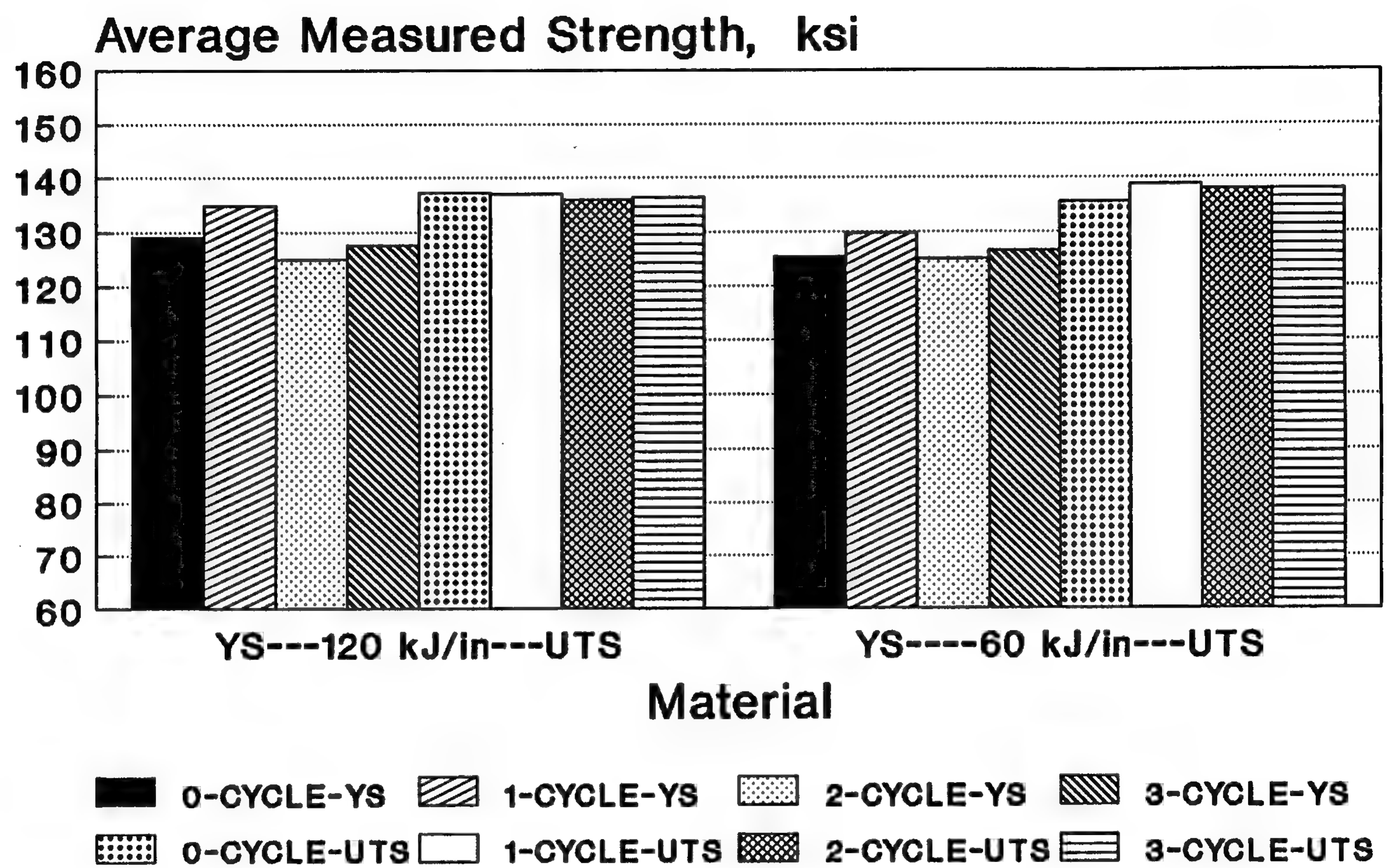

Figure 12. Effect of Gleeble thermal cycle on the strength of as-welded 8026C ULCB metal, GTAW.

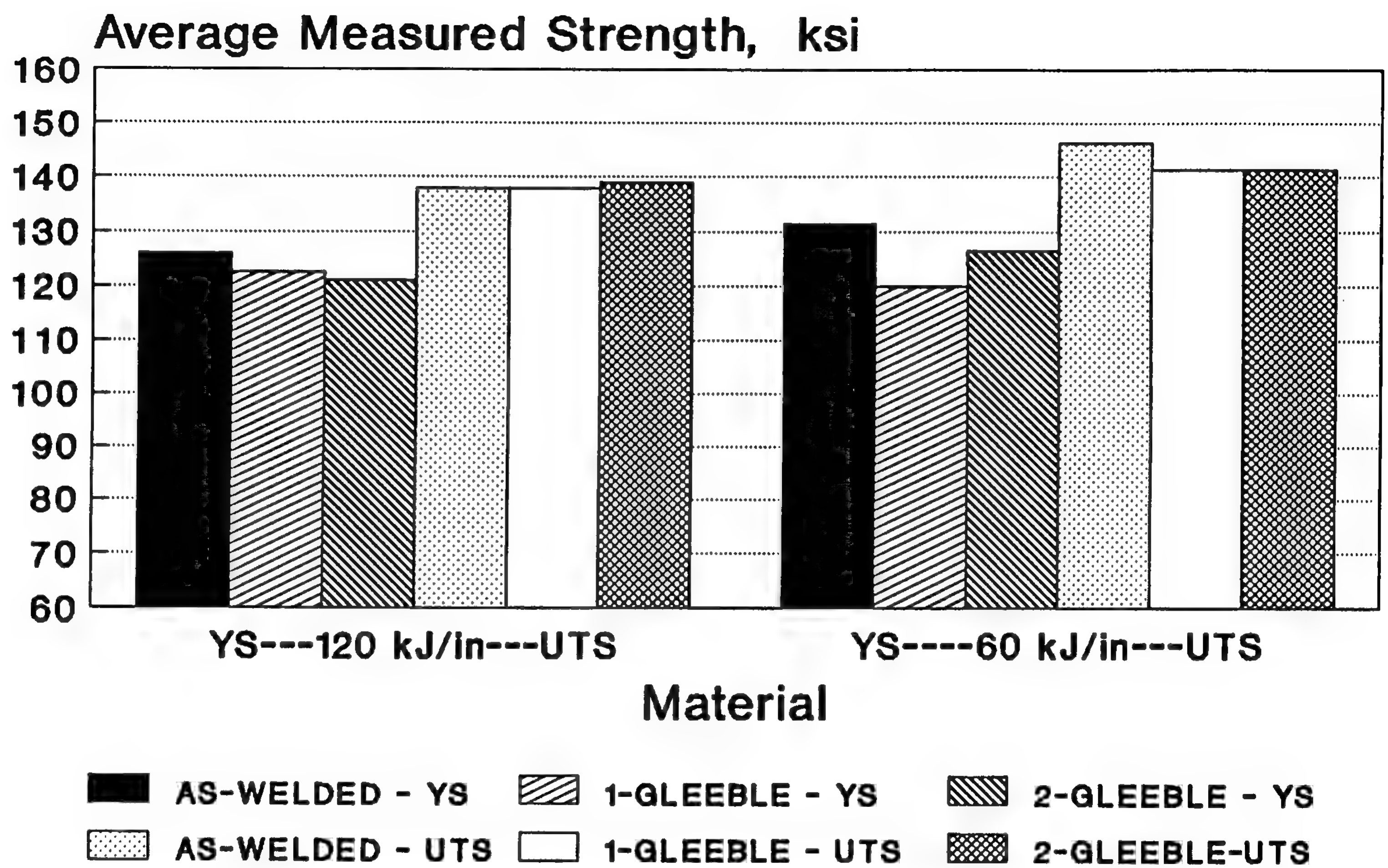

Figure 13. Effect of Gleeble thermal cycle on the strength of as-welded 8032C ULCB metal, GTAW.

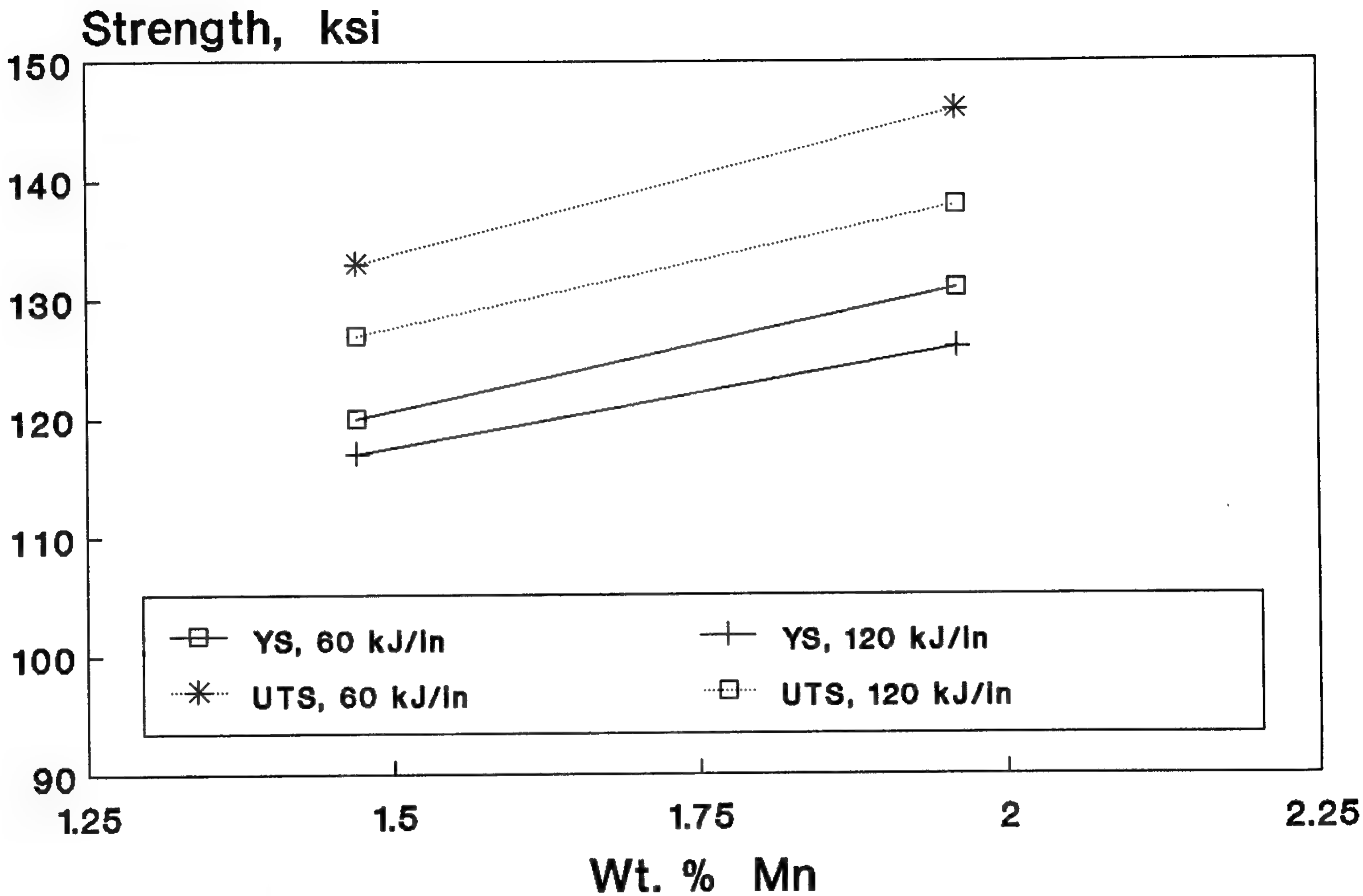

Figure 14. Effect of manganese on the strength of ULCB steel with 2.5% molybdenum - 3.4% nickel.

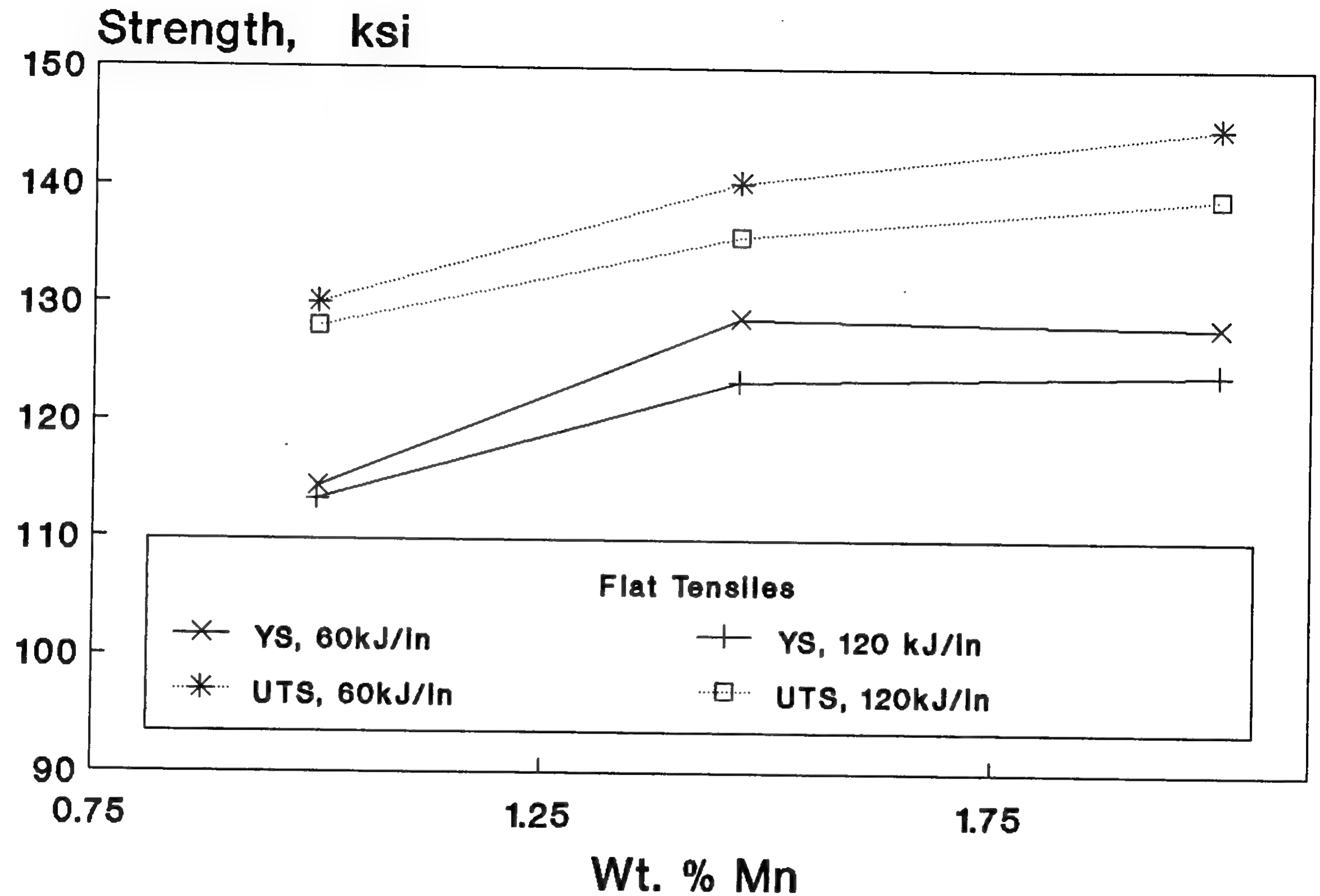

Figure 15. The effect of Manganese on the strength of ULCB steel with 3.5% molybdenum - 3.3% nickel.

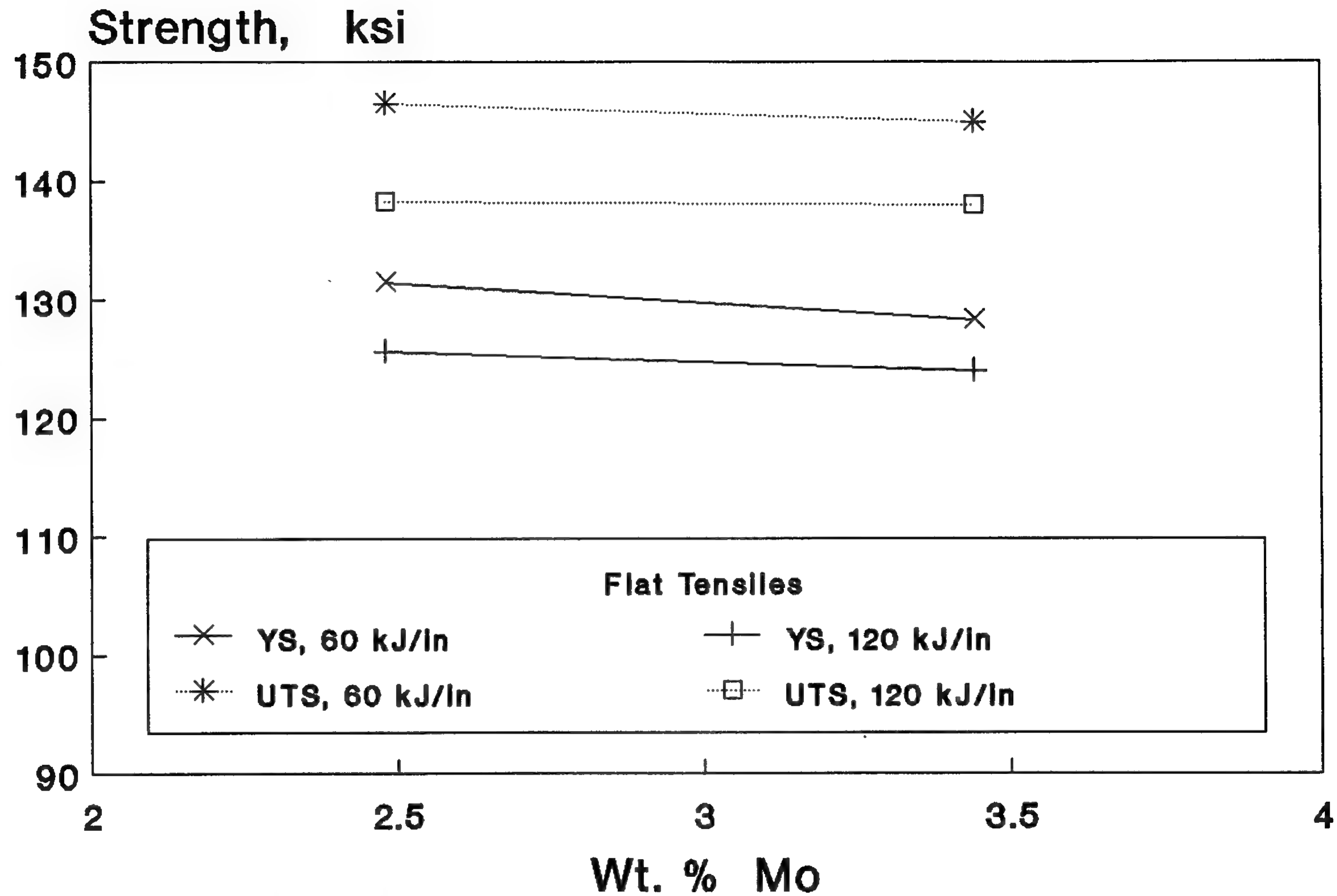

Figure 16, Effect of molybdenum on strength of ULCB steel with 2% manganese - 3.4% nickel.

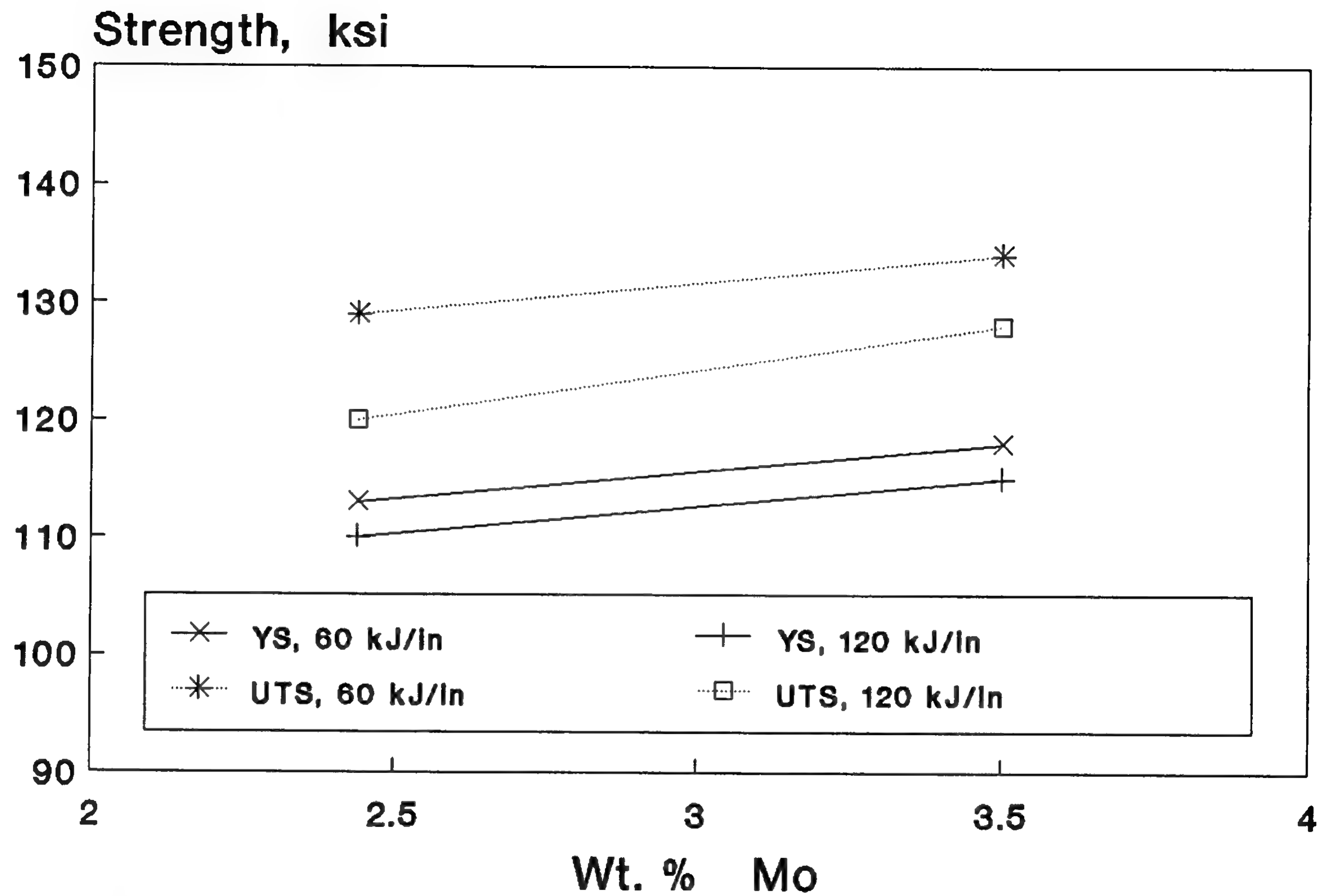

Figure 17. Effect of molybdenum on the strength of ULCB steel with 2.5% nickel - 1.4 manganese.

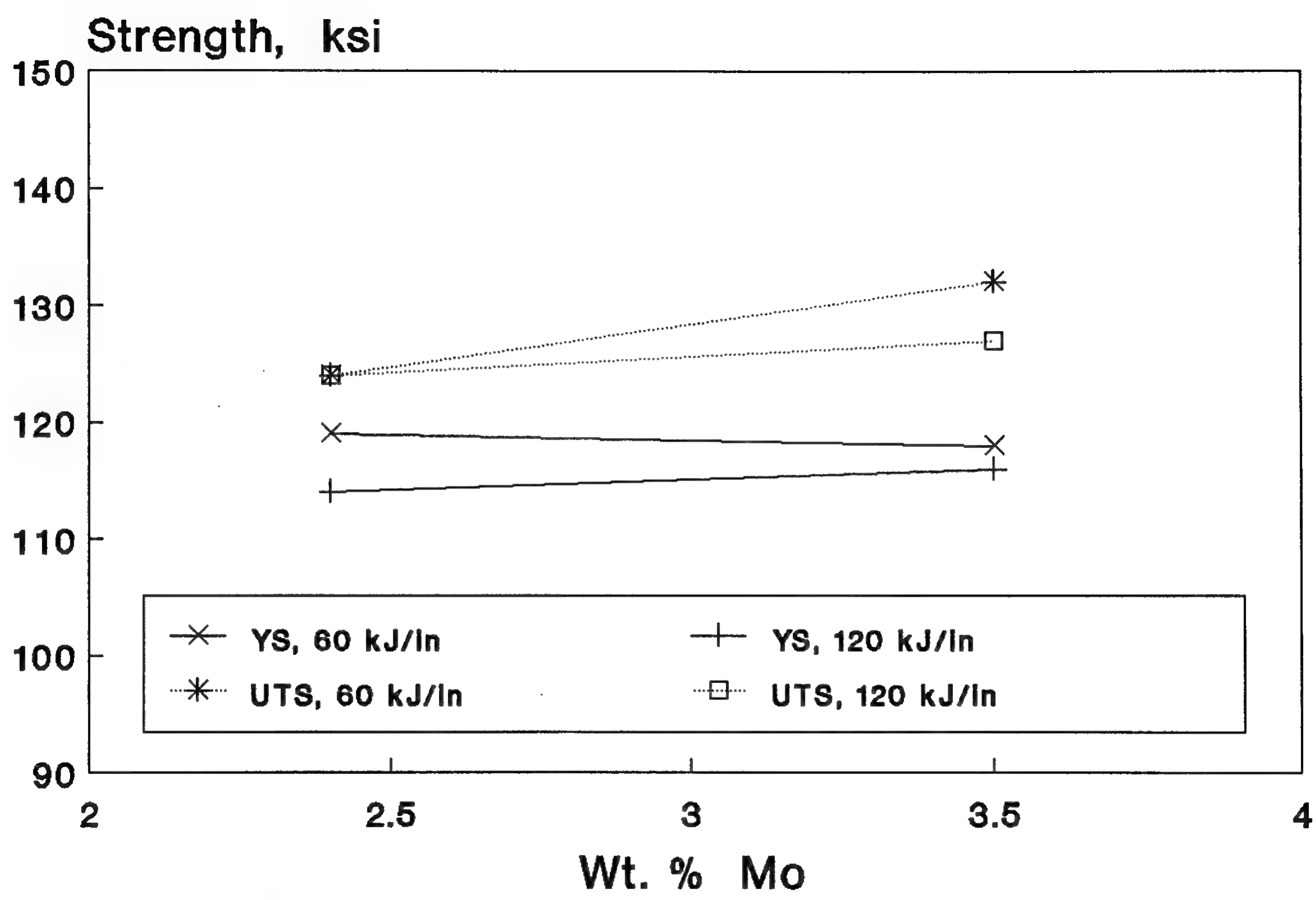

Figure 18. Effect of molybdenum on strength of ULCB steel with 3.5% nickel-1.4% manganese.

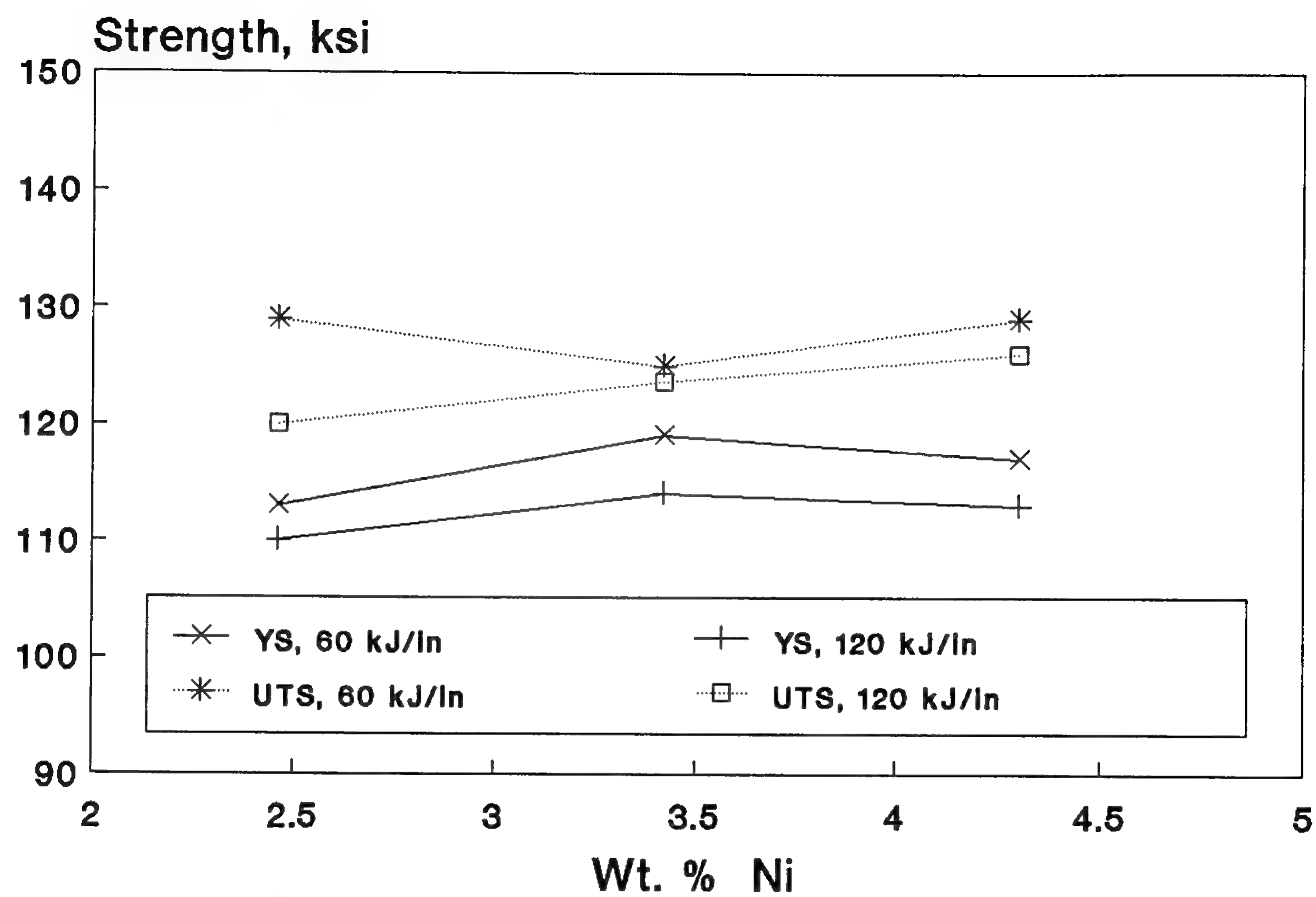

Figure 19. Effect of nickel on strength of ULCB steel with 2.4% molybdenum - 1.4% manganese.

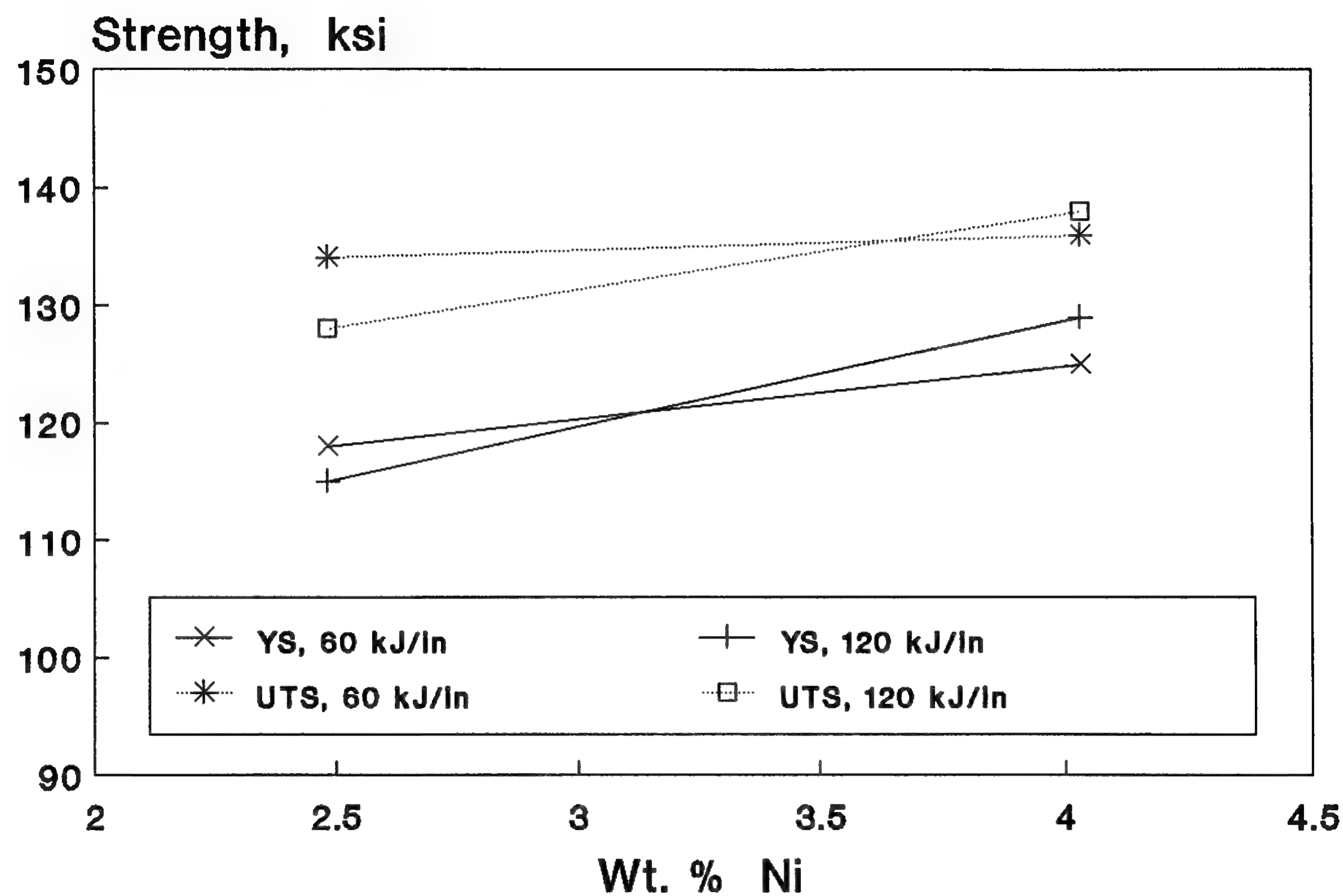

Figure 20. Effect of nickel on strength of ULCB steel with 3.5% molybdenum - 1.4 manganese.

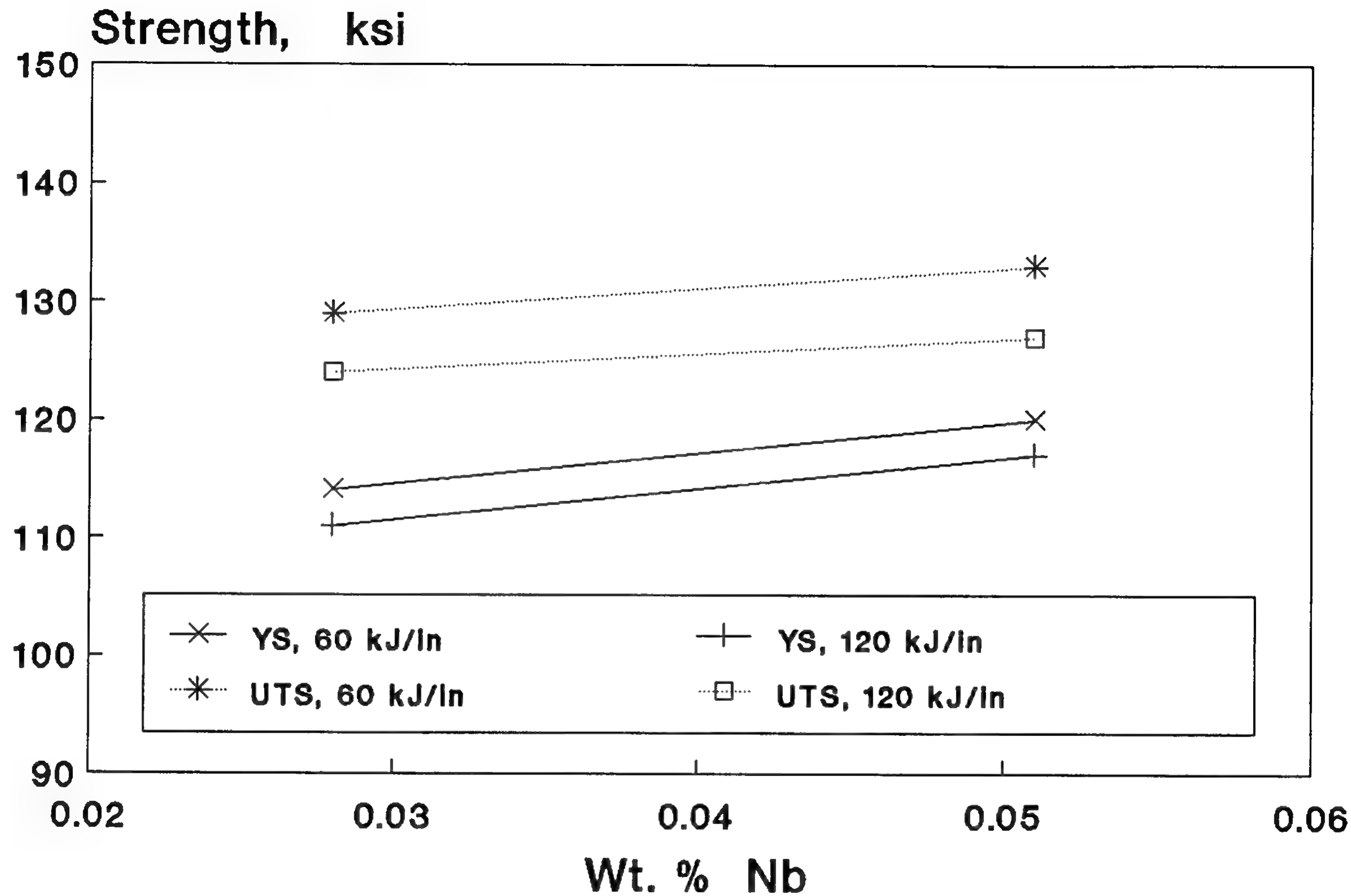

Figure 21. Effect of niobium on the strength of ULCB steel with 3.4% nickel-2.4% molybdenum-1.4% mang.-0.015 carbon.

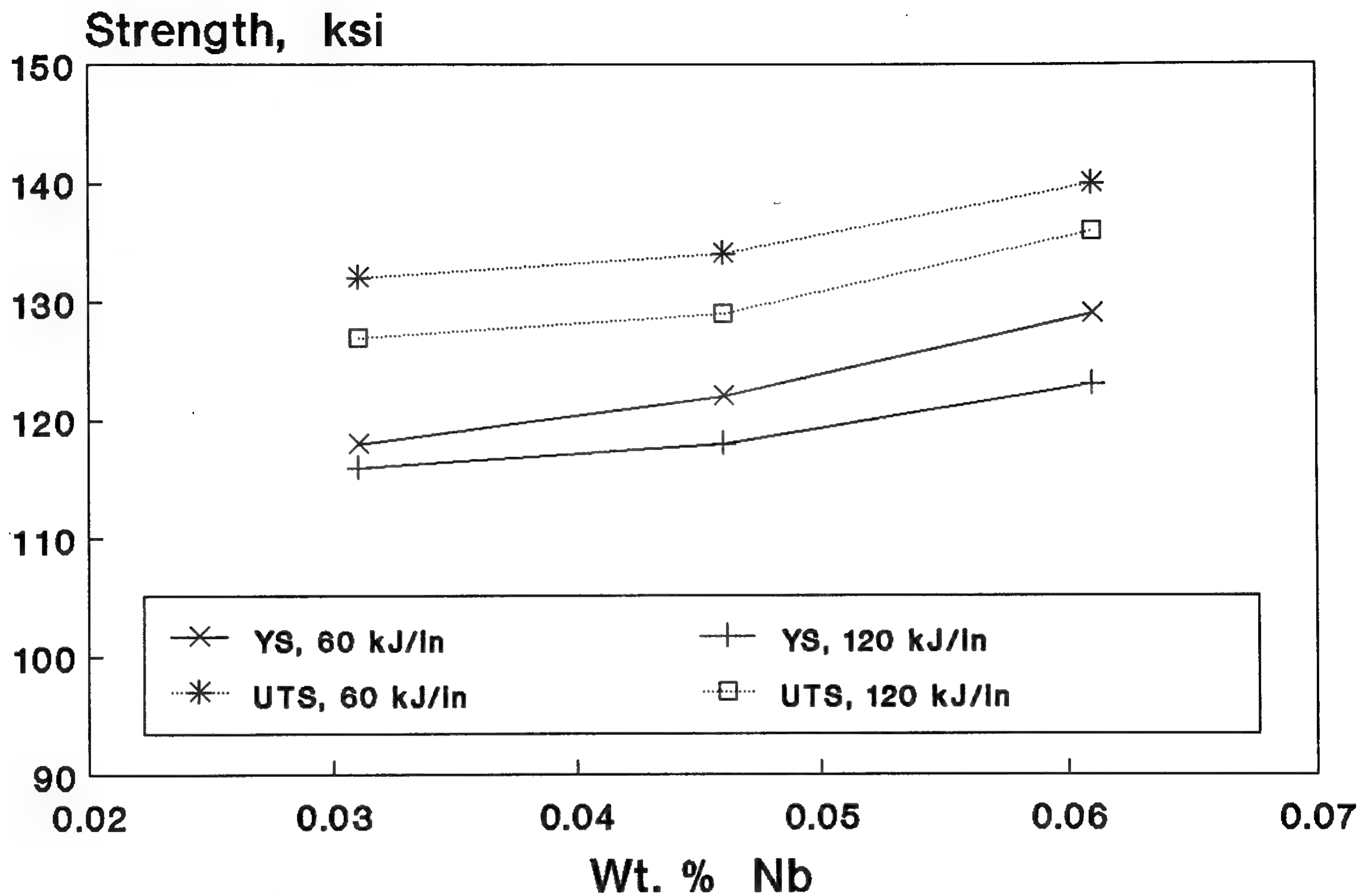

Figure 22. Effect of niobium on the strength of ULCB steel with 3.4% nickel-3.4% molybdenum - 1.4% manganese.

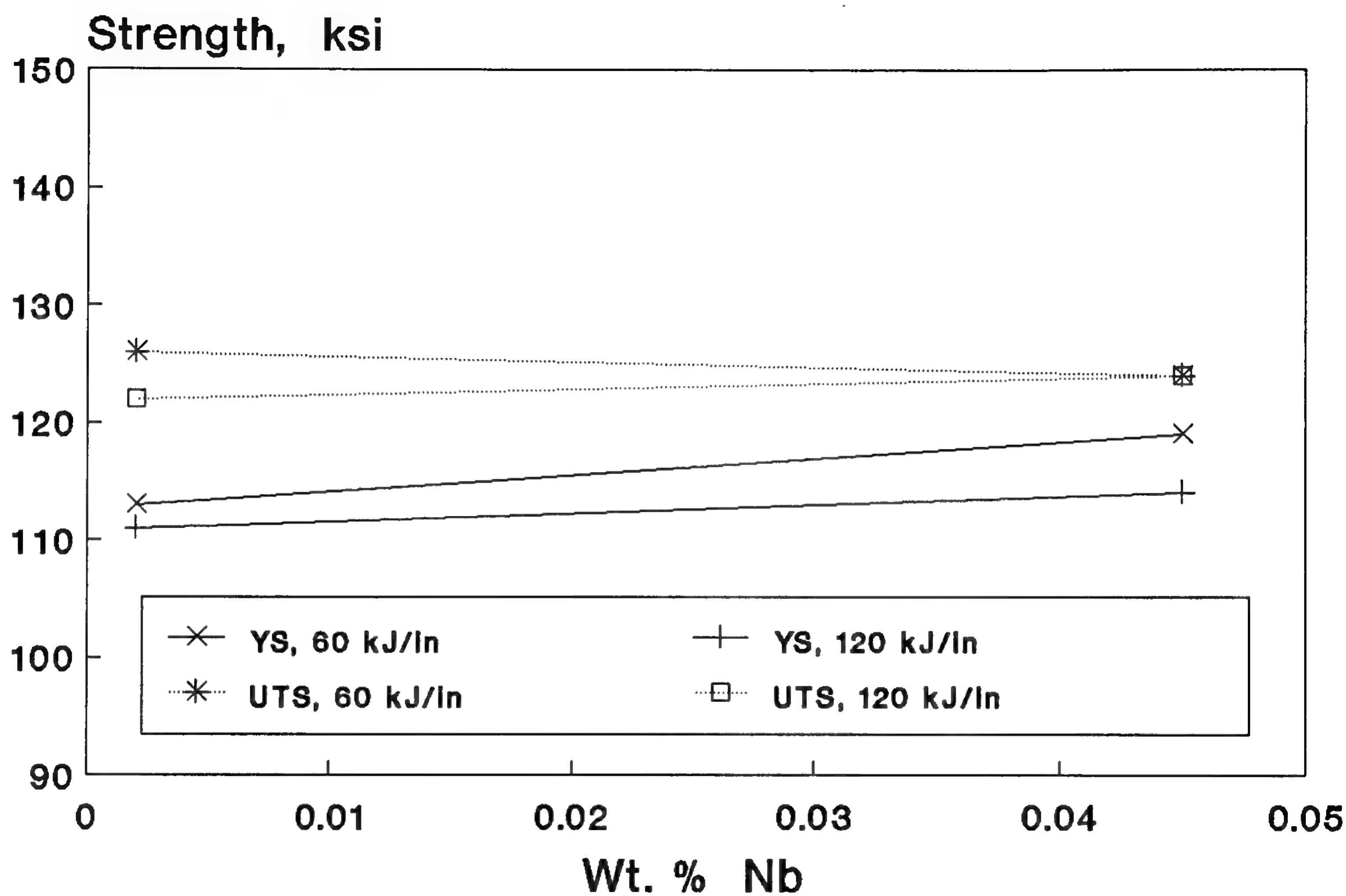

Figure 23. Effect of niobium on the strength of ULCB steel with 3.5% nickel-2.3% molybdenum-1.5% mang.-0.015 carbon.

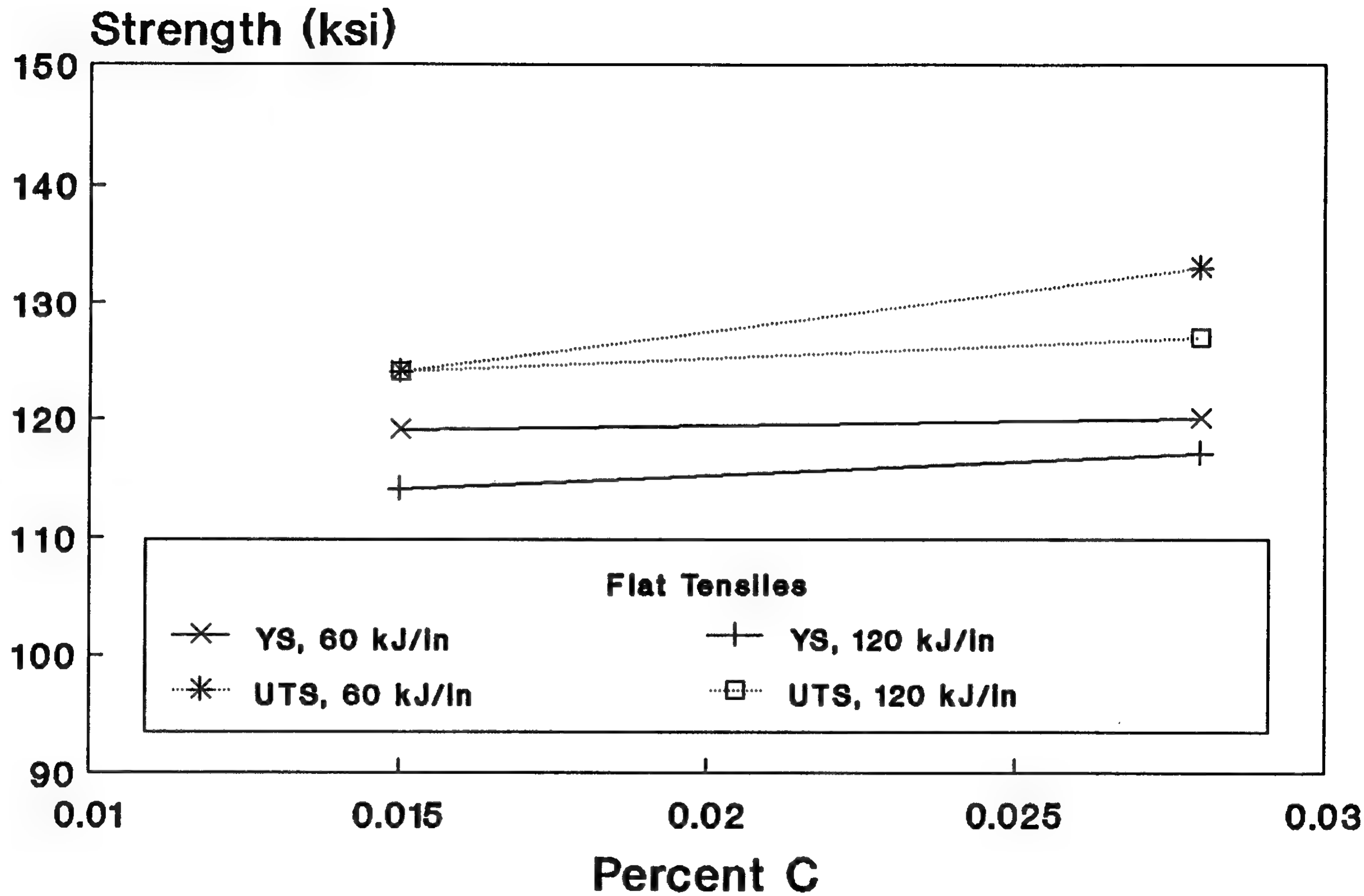

Figure 24. Effect of carbon on the strength of ULCB steel with 3.4% nickel-2.3% molybdenum - 1.4% manganese.

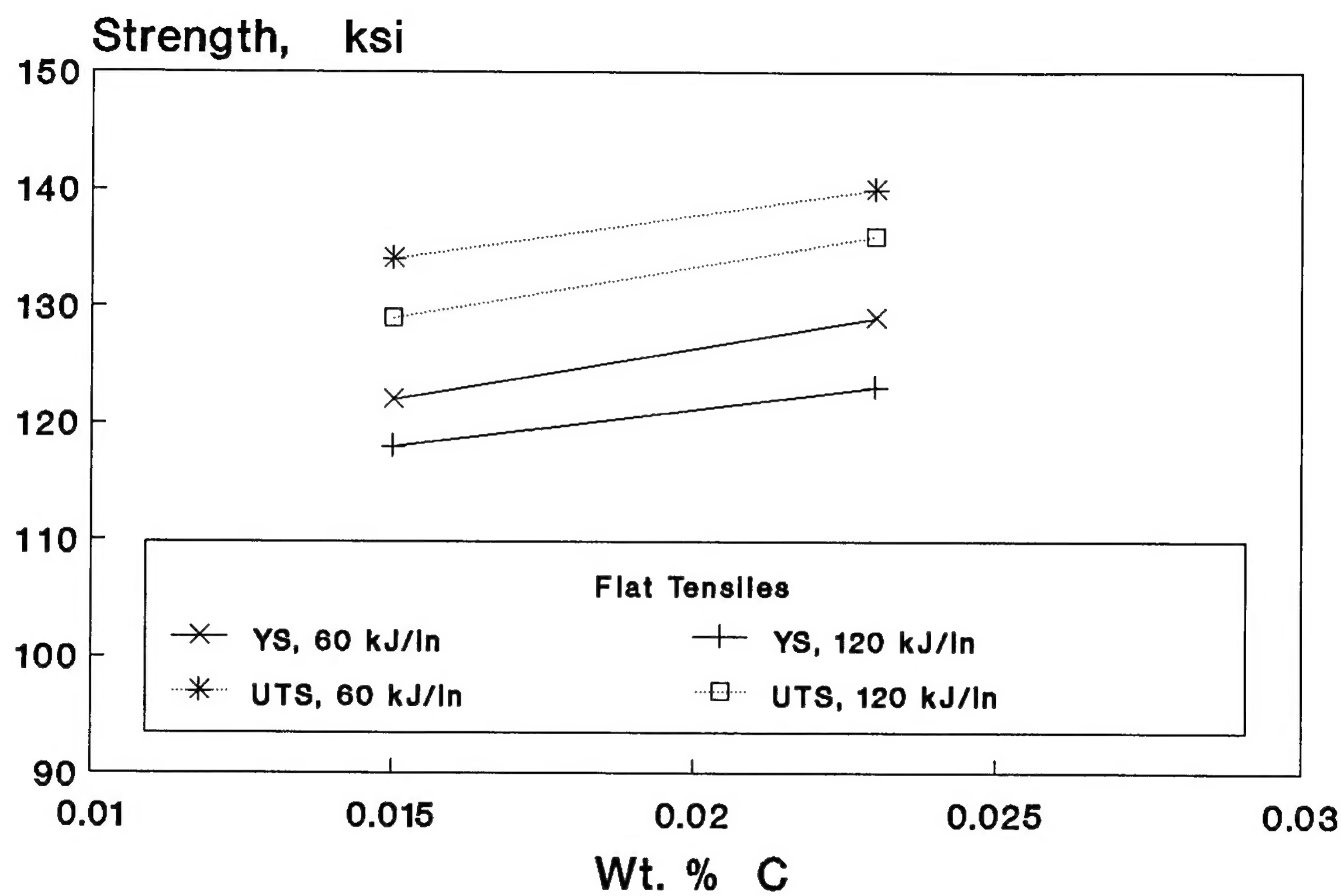

Figure 25. Effect of carbon on the strength of ULCB steel with 3.5% nickel-3.5% molybdenum - 1.4% manganese.

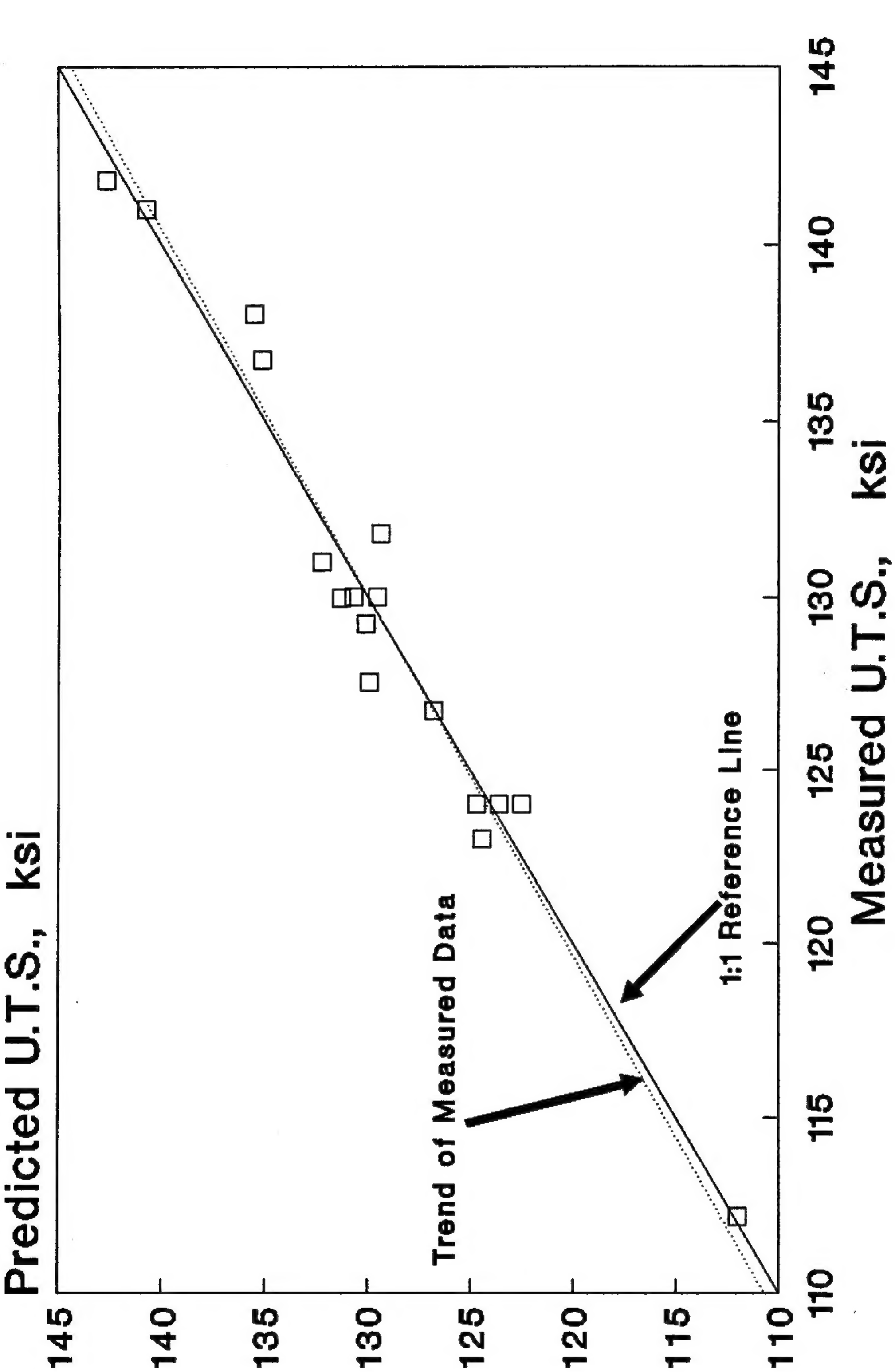

Figure 26. Measured Versus Predicted Ultimate Tensile Strength for ULCB Steel Welds from linear regression analysis.

INITIAL DISTRIBUTION

Copies			
1	OCNR		
	1	Code 225	
7	NAVSEA		
	1	SEA 03M	
	1	SEA 03M2	
	1	SEA 03P	
	1	SEA 03P1	
	1	SEA 03P2	
	1	SEA 03P4	
	1	SEA 99612	
5	DRPM		
	1	PMS 312	
	1	PMS 350	
	1	PMS 392	
	1	PMS 393	
	1	PMS 400	
12	DTIC		

Copies	Code
1	0115
1	60
1	601
1	602
1	603
1	61
1	61s
1	61.1
1	612
1	613
1	614
1	615
1	615 (Blackburn)
1	615 (DeLoach)
1	615 (Franke)
5	615 (Vassilaros)
1	615 (Wong)
1	62
1	63
1	64
1	65
1	66
1	67
1	68
1	69

REPORT DOCUMENTATION PAGE

Form Approved
OMB No. 0704-0188

1. AGENCY USE ONLY *(Leave blank)*	2. REPORT DATE	3. REPORT TYPE AND DATES COVERED
	March 1994	

4. TITLE AND SUBTITLE
The Effects of Alloying Elements on the Strength and Cooling Rate Sensitivity of Ultra-Low Carbon Alloy Steel Weld Metals

5. FUNDING NUMBERS
Program Element 62234N
DN 507603
Work Unit 1–2815–559

6. AUTHOR(S)
M.G. Vassilaros

7. PERFORMING ORGANIZATION NAME(S) AND ADDRESS(ES)
Carderock Division
Naval Surface Warfare Center
Code 615
Bethesda, MD 20084–5000

8. PERFORMING ORGANIZATION REPORT NUMBER
CARDIVNSWC–TR–61—93/12

9. SPONSORING /MONITORING AGENCY NAME(S) AND ADDRESS(ES)
Carderock Division
Naval Surface Warfare Center
Code 615
Bethesda, MD 20084–5000

10. SPONSORING /MONITORING AGENCY REPORT NUMBER

11. SUPPLEMENTARY NOTES

12a. DISTRIBUTION / AVAILABILITY STATEMENT
Approved for public release; distribution is unlimited.

12b. DISTRIBUTION CODE

13. ABSTRACT *(Maximum 200 words)*

A study was conducted to evaluate the effect of weld cooling rate on the strength of autogenous GTAW deposited weld metal. The basic weld metal composition was based on a low carbon bainite metallurgical system. The weld metal yield strength goal was 130 ksi, needed to surpass the current HY–130 weld metal requirements. Vacuum Induction Melted (VIM) heats of steel were produced and processed into 3/4" thickness plates. The autogenous gas tungsten are welds (GTAW) on the parent steel plates were produced under two different heat input conditions. Tensile specimens were produced from the weldments; specimens from certain heats were subjected to gleeble thermal simulations of multi-pass welding conditions using the Gleeble 1500. All specimens were then evaluated for yield and ultimate tensile strength. From the data presented, it was found that the experimental compositions studied were less sensitive to cooling rate than current HY–130 welding consumables. The compositions tested approached the target yield strength of 130 ksi, but further work is necessary in this area.

14. SUBJECT TERMS	15. NUMBER OF PAGES
Weld metal, Low-carbon bainite, Strength	16. PRICE CODE

17. SECURITY CLASSIFICATION OF REPORT	18. SECURITY CLASSIFICATION OF THIS PAGE	19. SECURITY CLASSIFICATION OF ABSTRACT	20. LIMITATION OF ABSTRACT
Unclassified	Unclassified	Unclassified	

NSN 7540-01-280-5500

Standard Form 298 (Rev. 2-89)
Prescribed by ANSI Std. Z39-18